Re-evaluating the prompt fission neutron spectrum of spontaneously fissioning 252Cf

Neudecker, Denise; Kelly, Keegan John; Carlson, Allan D.; Pritychenko, Boris; Brown, David A.; Grosskopf, Michael John; Vander Wiel, Scott Alan; Haight, Robert Cameron; Capote, R.; Massey, T.; Trkov, A.; Walton, Noah Anthony Wy

To be published in: EPJ Nuclear Sciences & Technologies

DOI to publisher's version: 10.1051/epjn/2025061

EPJ Nuclear Sci. Technol. **11**, 70 (2025)

https://doi.org/10.1051/epjn/2025061

EPJ Nuclear Sciences & Technologies

Available online at:
https://www.epj-n.org

REGULAR ARTICLE

OPEN ACCESS

Re-evaluating the prompt fission neutron spectrum of spontaneously fissioning ^{252}Cf

D. Neudecker[1,*], K.J. Kelly[1], A.D. Carlson[2,3], B. Pritychenko[3], D. Brown[3], M.J. Grosskopf[1], S.A. Van der Wiel[1], R.C. Haight[1], R. Capote[4], T.N. Massey[5], A. Trkov[6], and N.A.W. Walton[1,7]

[1] Los Alamos National Laboratory, Los Alamos, NM 87545, USA
[2] National Institute of Standards and Technology, Gaithersburg, MD 20899, USA
[3] Brookhaven National Laboratory, Upton, NY 11973, USA
[4] International Atomic Energy Agency, A-1400 Vienna, Austria
[5] Ohio University, Athens, OH 45701, USA
[6] Jožef Stefan Institute, Jamova 39, SI-1000 Ljubljana, Slovenia
[7] University of Tennessee, Knoxville, TN 37996, USA

Received: 17 June 2025 / Received in final form: 17 June 2025 / Accepted: 25 August 2025

Abstract. The prompt fission neutron spectrum (PFNS) of spontaneously fissioning ^{252}Cf is a Neutron Data Standards observable. Nearly all fission spectra of actinides were measured relative to it, using efficiencies derived from it, or analyzed with simulations validated by it. The current Standards evaluation was published by W. Mannhart in 1987. It could not be updated because the evaluation input, experimental mean values and covariances, were lost. First, we attempt to reproduce it. However, Mannhart's evaluation can only be reproduced within its one-σ uncertainties as some of its aspects (e.g., experimental covariances, rejected data points) remain unknown. Therefore, a new evaluation is presented: We revisit all existing experimental ^{252}Cf(sf) PFNS data, including those published after the release of the current Standards evaluation, and re-estimate associated covariances. The newly evaluated ^{252}Cf(sf) PFNS differs distinctly from Mannhart's below 300 keV and extends it to lower and higher outgoing neutron energies (500 eV–25 MeV). The new evaluated uncertainties are larger from 3–9 MeV and smaller otherwise. Spectrum averaged cross sections of importance to the International Reactor Dosimetry and Fusion File community calculated with the new spectrum are close to those calculated with Mannhart's evaluation and agree with experimental values well within their uncertainties.

1 Introduction

When a nucleus fissions, neutrons are emitted either on prompt or delayed time scales – the latter meaning after the on-set of beta decay. The prompt fission neutron spectrum (PFNS) is the energy distribution of neutrons promptly produced during or after an actinide fissions. Evaluated nuclear data of the PFNS of actinides are needed as input for particle transport codes to simulate fission-application quantities for subject areas ranging from reactor physics to nuclear criticality safety. Models frequently used for evaluating PFNS nuclear data [1–5] rely on accurate and precise experimental PFNS data. For many isotopes, over 70% of experimental PFNS data sets in the EXFOR[1] database [6] are measured relative to or use an evaluated ^{252}Cf(sf) PFNS for part of their analysis (e.g., to define the detector response or validate its simulation). Hence, any changes in the evaluated ^{252}Cf(sf) PFNS will have a direct impact on evaluated mean values of the PFNS of many other actinides. Also, if evaluated ^{252}Cf(sf) PFNS uncertainties increase or decrease, evaluated PFNS uncertainties of other actinides will increase or decrease along with them. Thus, changes in the ^{252}Cf(sf) PFNS uncertainties will impact uncertainties of application quantities of interest that are calculated with fission spectra of other nuclei.

Given that so many PFNS measurements make use of the ^{252}Cf(sf) PFNS as a reference, and because it has been measured to high precision by several groups, it is a

[1] EXFOR, for EXchange FORmat, is a low- and intermediate-energy nuclear reaction data library. The experimental data stored in this database provide key input for nuclear data evaluations.

* e-mail: dneudecker@lanl.gov

Standards observable; its evaluated nuclear data are provided by the Neutron Data Standards project coordinated by the International Atomic Energy Agency (IAEA) [7]. Also, the ^{252}Cf(sf) PFNS is important for the neutron dosimetry community since it is used to validate cross section evaluations of dosimetry reactions by comparing calculated ^{252}Cf(sf) spectrum averaged cross sections (SACS) versus measured values. In addition to that, model codes predicting PFNS distributions, such as those in Refs. [8–10], are often benchmarked using the evaluated and experimental ^{252}Cf(sf) PFNS. Finally, neutron detector efficiencies are often deduced using a ^{252}Cf source. Hence, a detailed understanding of evaluated ^{252}Cf(sf) PFNS nuclear data is of importance for many applications.

The current ^{252}Cf(sf) PFNS Standards evaluation was provided by W. Mannhart and published in 1987 [11]. Unfortunately, it cannot be reproduced, because the evaluation input data (mean values and covariances of experimental data) were lost. While the executable of the evaluation code is still available, the code itself is not. However, at least seven new experimental ^{252}Cf(sf) data sets have been published since the evaluation was undertaken [12–18]. As one cannot update the current ^{252}Cf(sf) PFNS Standards values, these new experimental data sets could not be easily incorporated in Mannhart's evaluation to further our understanding of this observable.

We describe an effort by the AIACHNE (AI/ML Informed cAlifornium CHi Nuclear data Experiment) project to render the Mannhart ^{252}Cf(sf) PFNS evaluation [11] reproducible again and to produce a new evaluation. This was accomplished by surveying the experimental mean values and standard deviations used as input, and retracing the steps of Mannhart's evaluation. We acknowledge that certain aspects of the evaluation remain unknown: For instance, no documentation on correlations of input experimental data exists. Also, we do not know which specific data points of individual experiments were rejected by Mannhart. Still, the evaluation we obtain reproduces Mannhart's evaluated data well within the one-σ evaluated uncertainties obtained by Mannhart, that is within 0.04–3.4% above 25 keV as shown in Section 4.

In a second step, we reviewed all experimental data available for the ^{252}Cf(sf) PFNS, including those reported after the Mannhart evaluation, and developed a new evaluation.

Section 2 shows the evaluation algorithm employed and how it differs from the approach used by W. Mannhart in Ref. [11]. Section 3 discusses which input data were used for the new evaluation and the reasoning behind adopting or rejecting data sets that were used for Mannhart's Standards ^{252}Cf(sf) PFNS. The new evaluation is described in Section 4. This new evaluation has less structures below 300 keV and has a larger energy range than Mannart's evaluation. As it is similar from 300 keV to 12.8 MeV, SACS calculated from the new ^{252}Cf(sf) PFNS evaluation are close to those calculated with Mannhart's spectrum. Section 5 provides a short summary and outlook.

2 Methods

2.1 Evaluation algorithm

Mannhart used the generalized least squares algorithm [19,20] to evaluate the ^{252}Cf(sf) PFNS on a grid of 70 energies [11,21]. This algorithm yields a vector of evaluated PFNS, χ', and an associated covariance matrix, $\mathbf{Cov}^{\chi'}$, by:

$$\begin{aligned}\chi' &= \chi + \mathbf{Cov}^{\chi'}(\mathbf{S})^t(\mathbf{Cov}^N)^{-1}(\mathbf{N}-\mathbf{S}\chi)\,,\\ \mathbf{Cov}^{\chi'} &= \mathbf{Cov}^{\chi} - \mathbf{Cov}^{\chi}(\mathbf{S})^t\mathbf{Q}^{-1}\mathbf{S}\mathbf{Cov}^{\chi},\end{aligned} \tag{1}$$

with

$$\mathbf{Q} = \mathbf{S}\mathbf{Cov}^{\chi}(\mathbf{S})^t + \mathbf{Cov}^N. \tag{2}$$

The matrix $\mathbf{Cov}^N$ is the covariance matrix associated with the vector of all experimental ^{252}Cf(sf) PFNS, $\mathbf{N}$. The vector χ and matrix $\mathbf{Cov}^{\chi}$ are the prior PFNS and covariances. It is unclear what Mannhart used for these, as summarized in Table 1, but it was likely chosen to be an uninformative prior that would not have influenced the evaluation. The design matrix $\mathbf{S}$ and its transpose $(\mathbf{S})^t$ were set by Mannhart to unity when the experimental data are on the same grid point as the evaluated PFNS, otherwise the matrix entries were zero. In Refs. [4,5] linear interpolation is used for obtaining $\mathbf{S}$. This interpolation was avoided by Mannhart by interpolating $\mathbf{N}$ onto the grid of χ' and χ where he defined the slope of the data by using Maxwellian functions fit separately to data from each experiment [21]. Unfortunately, it remains somewhat unclear how $\mathbf{Cov}^N$ were transformed to the evaluation grid. Mannhart states in Ref. [22] that the statistical uncertainties were transformed to the new grid while: "the systematic components and their correlations influenced the data adjustment process in its entirety". We tried to reproduce the Maxwellian fit parameters in Table 3 of Ref. [11], but could only reproduce a few of them which points to a small mistake in the original fitting procedure. Mannhart writes that the impact of transforming the data onto the evaluation grid was almost negligible in Ref. [11], and so would be any mistake in the fitting procedure.

In Ref. [3,23], it is recommended to treat experimental PFNS as shape data. This recommendation means that one adopts the overall shape of the data but the data set as a whole can be scaled up or down with one constant multiplicative factor to better align with other data sets or the prior PFNS. However, Mannhart treated the data of Dyachenko et al.[2] [24,25], Böttger et al. [26–29], and Märten et al. [30–34] as absolute data, meaning that the scaling was kept fixed during the evaluation. The scaling constants of other data sets were obtained as part of the evaluation: Poenitz and Tamura data [35,36] were renormalized by a factor of 1.007, Blinov et al. [37–39] by 0.997, Boldeman et al. ^{6}Li data by 1.009, and Boldeman plastic scintillator PFNS by 1.01 [40]. When we try to reproduce

[2] The data set identified as "Lajtai et al." by Mannhart correspond to data stored in EXFOR under the first author Dyachenko (EXFOR accession number 40875.002). We will henceforth name this data set as Dyachenko.

Table 1. Known and unknown aspects of Mannhart's evaluation. The unknowns impacting the evaluation the most are highlighted in bold font.

Aspect	Known	Unknown
Code	GLS wihout PPP correction	Actual code lost
Prior	Grid points	Mean values and covariances
$\{\mathbf{N}, \mathrm{Cov}^N\}$	**N** & uncertainties read from plots	**Correlations**
Rejected data	No. of rejected points	**Exact datapoints rejected**
S	Transformation procedure	Maxwellian fit parameters not reproducible

Mannhart's evaluation, these scaling factors are considered along with treating the same data as absolute as Mannhart did.

χ' and $\mathbf{Cov}^{\chi'}$ must be normalized after the evaluation to satisfy the ENDF-6 format requirement on the PFNS [41] that results from the PFNS being a probability distribution function: the integral over an outgoing energy range where the PFNS is non-negligible must be unity. As a result, the rows and columns of the covariance matrix must sum, within a limit defined by numerical precision, to zero. These normalization conditions can be enforced with algorithms presented in equations (11)–(13) of [5], equations (3)–(6) in Ref. [42], or in equations (7) and (8) of Ref. [21].

The algorithm for the new evaluation presented here differs from Mannhart's evaluation in that all experimental PFNS are treated as shape data. As a prior, we use Mannhart's pointwise evaluated PFNS and a diagonal covariance matrix with 100% uncertainty. In addition to that, we employ the iteratively reweighted least squares (IRLS) algorithm [43] to address an effect termed "Peelle's Pertinent Puzzle" (PPP) where one obtains an evaluated mean value outside of the range of two highly-correlated input data [44,45]. The issue arises because one improperly formulates covariances relative to the measured value rather than the best estimate of the observable at hand. Following Ref. [43], IRLS treats PPP by assuming a best guess for the observable to be evaluated, χ', starting with the prior χ. The experimental covariance matrix is then recalculated such that each matrix element is given by $\mathrm{Cov}^{N,(0)}_{i,j} = \mathrm{Cov}^{N}_{i,j}\chi_i\chi_j/(N_iN_j)$. Then, one executes Equation (1) with $\mathbf{Cov}^{N,(0)}$ to obtain the evaluated PFNS $\chi'^{(1)}$ in the first iteration. That is then used to transform $\mathrm{Cov}^{N,(1)}_{i,j} = \mathrm{Cov}^{N}_{i,j}\chi'^{(1)}_i\chi'^{(1)}_j/(\chi_i\chi_j)$ for evaluating $\chi'^{(2)}$. This iterative procedure is executed until convergence is reached, i.e., until $\chi'^{(n)}$ differs negligibly, that is by less than 10^{-7}, from $\chi'^{(n+1)}$. IRLS was implemented in the code ARIADNE [46] to give new evaluated χ'.

2.2 Uncertainty quantification methods for input data

The experimental covariances $\mathbf{Cov}^N$ were estimated based on vectors of partial uncertainties, δ^k, for distinct and independent uncertainty sources k, and correlation coefficients, $\mathrm{Cor}^k_{i,j}$, for each partial uncertainty source k of the PFNS at outgoing neutron energies E_i and E_j. The total covariance elements, $\mathrm{Cov}^N_{i,j}$, were then obtained from this information via:

$$\mathrm{Cov}^N_{i,j} = \sum_k \delta^k_i \mathrm{Cor}^k_{i,j}\delta^k_j + \mathrm{Cov}^{\Delta t}_{ij} + \mathrm{Cov}^{\Delta l}_{ij}, \quad (3)$$

where $\mathrm{Cov}^{\Delta t}_{ij}$ and $\mathrm{Cov}^{\Delta l}_{ij}$ are experimental covariances stemming from the time resolution, Δt, and time of flight (TOF) length uncertainty, Δl. The latter covariances are estimated following the procedure outlined in equation (2) of [46]. This uncertainty procedure requires a Maxwellian temperature, T, that best describes the data. If this value was not provided by the experimenters, we assume a temperature of $T = 1.42\,\mathrm{MeV}$ which corresponds to a PFNS average energy of $\frac{3}{2}T = 2.13\,\mathrm{MeV}$. One also needs to know the TOF length l that is listed in Table 2.

Values for δ^k, Δt, and Δl were mostly retrieved from EXFOR entries or the literature of the data set at hand. The time resolution, Δt, is often the dominant uncertainty source at high outgoing neutron energies. In Table 2, Δt are listed for the individual experiments. At low outgoing neutron energies, background, multiple scattering, and counting statistics uncertainties are the main contributors to $\mathbf{Cov}^N$. Values for $\mathrm{Cor}^k_{i,j}$ are estimated following Table 2 of Ref. [47]. All $\mathbf{Cov}^N$ for data sets listed in Table 2 were estimated with the code ARIADNE [46], and are provided as supplemental material.

2.3 Validation with spectrum averaged cross sections

The International Reactor Dosimetry and Fusion File II (IRDFF-II) project [48] provides an extensive set of evaluated cross sections, $\sigma(E)$, with full covariances between the cross sections, $\mathrm{Cov}^{\sigma}(E, E')$, which can be used to validate normalized ^{252}Cf(sf) PFNS. The validation is undertaken by comparing spectrum averaged cross section, SACS, calculated in a given spectrum with experimental SACS. A spectrum averaged cross-section, $\langle\sigma\rangle$, is defined as an integral of a cross section in a neutron field $\phi(E)$:

$$\langle\sigma\rangle = \int_{10^{-5}\,\mathrm{eV}}^{30\,\mathrm{MeV}} \mathrm{d}E\phi(E)\sigma(E), \quad (4)$$

where $\sigma(E)$ are the evaluated cross sections from IRDFF-II. The variable $\phi(E)$ denotes the normalized ^{252}Cf(sf) PFNS χ' such that

$$\int_{10^{-5}\,\mathrm{eV}}^{30\,\mathrm{MeV}} \mathrm{d}E\phi(E) = 1, \quad (5)$$

Table 2. Experimental data used within this work are identified via the name of the first author, publication year of the first reference in EXFOR, and their EXFOR accession number. The fission detector type, fission-detector efficiency (ε_f), neutron detector type ("SCIN" is short for scintillator, "IOCH" for ionization chamber, "GSD" for gas scintillation detector, "FISCH" for fission chamber, and "GLASD" for glas detector), angle between normal to the sample and detector ($\angle$), neutron-detector efficiency (ε_n), neutron detector size (NDS, with diameter × height or thickness), sample activity (α), sample diameter ($\varnothing$), sample backing material (SBM with "St. steel" for stainless steel), sample backing thickness (SBT), TOF length (l), and time resolution (Δt) are also listed. If "?" is given in the Table, the value was not found for that particular data set. The values in brackets and italics for Kornilov PFNS were found as part of the revision process.

Name, Year	EXFOR #	Fission detector	ε_f (%)	Neutron detector	$\angle$ (°)	ε_n (%)	NDS (cm)	α (10^4f/s)	$\varnothing$ (mm)	SBM	SBT (mm)	l (cm)	Δt (ns)
Blinov, 1980	40535.002	SCIN	?	^{6}Li-I(Eu) crystal	?	?	1.8×0.2, 0.4	2, 9.8	40	Pt	0.1	6.25	1.5
Blinov, 1980	40535.003	SCIN	?	^{6}Li-I(Eu) crystal	?	?	1.8×0.2, 0.4.	2, 9.8	40	Pt	0.1	12.5	1.5
Blinov, 1980	40535.004	SCIN	?	^{6}Li-I(Eu) crystal	?	?	1.8×0.2, 0.4	2, 9.8	40	Pt	0.1	25	1.5
Blinov, 1980	40535.005	SCIN	?	^{6}Li-I(Eu) crystal	?	?	1.8×0.2, 0.4.	2, 9.8	40	Pt	0.1	50	1.5
Blinov, 1973	40418.007	IOCH	99	^{235}U(n,f) IOCH	45	80	$10 \times ?$	45.1	40	Pt	0.1	50	1.32
Böttger, 1983	None yet	2 × IOCH	95.4 99.5	NE-213 SCIN	0, 12.5, 25, 37.5	20	25.4×5.08	11, 16	5, 15	Au, Pt	?	1200	1.5
Boldeman, 1986	30775.002	IOCH	97	NE-102 plastic SCIN	?	97	5.08×2.54	5–8	?	St. steel	?	301.5	2.6–3
Boldeman, 1986	30775.003	IOCH	97	^{6}Li-glass SCIN	?	97	5.08×0.254	4.4	?	St. steel	?	40	2.6–3
Boytsov, 1983	40874.002	IOCH	98 ± 2	Anthracene SCIN	0,45	?	1.8×0.4	6.5	20	St. steel	0.04	51	4.2
Boytsov, 1983	40874.003	GSD	97 ± 2	Thin-wall IOCH	0	80	10×0.8	20	?	Pt	0.01	51	4.5
Boytsov, 1983	40874.004	GSD	97 ± 2	Gas SCIN IOCH	0	?	11×0.01	20	?	Pt	0.01	51	2.5
Chalupka, 1990	22202.003 004+005	FISCH	99.5	NE-213 SCIN	0	20	25.4×5.08	15.6	15	Pt	?	279.6	1
Dyachenko, 1989	40875.002	FISCH	99	NE-912 ^{6}Li GLASD	0.0186	[24]	4.5×0.95	1	7	Pt	0.05	30	4
Kornilov, 2015	14431.002	IOCH	99	NE-213 SCIN	?	15–30	12.7×5.08	2.2–3.9	10	St. steel	?	*(423.8)*	*(2.4)*
Lajtai, 1990	41158.003	FISCH	99	NE-912 ^{6}Li GLASD	?	[14]	4.5×0.95	1	7	Pt	0.05	30	4
Märten, 1984	31854.002	FISCH	85.8 ± 1	NE-213 SCIN	0	?	12.7×12.7	3.4	?	Ta	0.125	450	2.0743
Märten, 1990	30969.002	IOCH	99.2	NE-213 SCIN	0	?	12.7×12.7	7	?	?	?	590.5	1.5
Märten, 1990	30969.003	IOCH	99.2	NE-213 SCIN	60	?	12.7×3.81	7	?	?	?	327.5	1.3
Poenitz, 1982	14278.002	SCIN	71	NE-213 SCIN	0	83–98	15.2×17.8	14.3	?	Pt	0.25	258	4
				NE-213 SCIN	0	77–96	20×37					347	4

where the integral limits correspond to the minimal and maximal energies of ϕ.

The IRDFF-II [48] project compiled a list of trusted experimental SACS and provides high-fidelity nuclear data evaluations for each reaction channel that are essential for the nuclear fission and fusion reactor metrology community. In addition, Tables 18 and 19 of Ref. [48] summarize comparisons of SACS experimental and calculated data. The calculated SACS were obtained with evaluated ^{252}Cf(sf) PFNS of Mannhart and IRDFF-II evaluated cross sections. These calculated IRDFF-II SACS are used here for counter-checking our SACS calculations using Mannhart's evaluated PFNS and IRDFF-II cross section to ensure that our calculation procedure is correct. Then, SACS using the new evaluated PFNS and IRDFF-II evaluated cross sections are computed. Finally, SACS are shown in Section 4 as a function of the energy, $E_{50\%}$, that is defined as the energy at which the reaction rate reaches 50%,

$$\frac{\int_{1e-5\,\mathrm{eV}}^{E_{50\%}} \mathrm{d}E\phi(E)\sigma(E)}{\int_{1e-5\,\mathrm{eV}}^{30\,\mathrm{MeV}} \mathrm{d}E\phi(E)\sigma(E)} = \frac{1}{2}. \tag{6}$$

The variances of the calculated SACS, $\Delta^2\langle\sigma\rangle$,

$$\Delta^2\langle\sigma\rangle = \int_{10^{-5}\,\mathrm{eV}}^{30\,\mathrm{MeV}} \int_{10^{-5}\,\mathrm{eV}}^{30\,\mathrm{MeV}} dEdE' \left[\phi(E)\mathrm{Cov}^{\sigma}(E,E')\phi(E') + \sigma(E)\mathrm{Cov}^{\phi}(E,E')\sigma(E')\right], \tag{7}$$

factor in IRDFF-II nuclear data cross-section covariances, $\mathrm{Cov}^{\sigma}(E,E')$, and normalized ^{252}Cf(sf) PFNS covariances, $\mathrm{Cov}^{\phi}(E,E')$ (i.e., after applying the normalization constraint to $\mathbf{Cov}^{\chi'}$), assuming that these two covariances are independent.

3 Input data for the evaluations

Data by six experimental teams were included in the evaluation by Mannhart [11], while this work includes data sets by nine teams. It can be seen from Table 3 that the data by first author Dyachenko [24,25] were replaced by those from Lajtai et al. [14] as the authors stated in Ref. [49] that errors were found in the Monte Carlo (MC) simulations of the detector efficiencies of [24,25]. A corrected detector efficiency was presented and applied to the same raw data in Ref. [14] which describes the data set we adopt for the new evaluation. Data by Märten et al. documented in various laboratory reports and one proceeding [30–34] were replaced by those published later by the same team in a journal publication [13]. We added a data set by the group of Blinov et al. [50] to those used by Mannhart [37–39], while we reject Boldeman et al. data [40] measured with a ^{6}Li neutron detector that showed a distinct bias at the location of the ^{6}Li(n,t) resonance. Lastly, we added data sets by Boytsov et al. [51,52], Chalupka et al. [15], and Kornilov [12] that were not included in Mannhart's evaluation. In general, all

Table 3. The data sets used for Mannhart's evaluation versus those selected for this work. Bold font is used to draw attention to changes in year, first author or detector selection.

Mannhart evaluation	This work
Blinov, 1973 [37–39]	Blinov, 1973 and **1980** [50]
Böttger, 1990 [26–29]	Böttger, 1990 [26–29]
Boldeman, 1986 (Li, plastic)	Boldeman, 1986 (**plastic**) [40]
Dyachenko, 1989 [24,25]	**Lajtai, 1990** [14]
Märten, 1984 [30–34]	Märten, **1990** [13]
Poenitz, 1983 [35,36]	Poenitz, 1983 [35,36]
–	Boytsov, 1983 [51,52]
–	Chalupka, 1990 [15]
–	Kornilov, 2015 [12]

^{252}Cf(sf) PFNS data sets in EXFOR were reviewed. Those not called out as accepted did not meet criteria set forth in Section 3.1 for including data into the evaluation.

Each data set is summarized on a high level below along with reasoning for including or replacing data for the new evaluation. Potential issues that could lead to biases in experimental data are also described. In addition, Table 2 provides a concise summary of important measurement details (detector types, Δt, etc.) to be able to easily compare the major aspects of each experiment.

3.1 Criteria for including experimental data into new evaluation

As the ^{252}Cf(sf) PFNS is a part of the Standards, a new evaluation must be of high fidelity. Consequently, the same applies to the input data for the evaluation. We applied the following selection criteria to the data:

- Only TOF measurements are used.
- Data must be corrected for backgrounds (typically, α-particle, γ-ray, random-coincidence, and shadow-bar backgrounds apply), scattering and attenuation (in the environment, detectors, and sample), fission and neutron detector response, decay of the sample for very long measurement times, fission fragment absorption in the sample, deadtime, and angular anisotropy of neutron emission relative to the fission fragment detection.
- If no correction was undertaken for a specific effect, it must be conceivable that its impact on the experimental PFNS was minimal. If that is not the case and it would only concern an isolated outgoing-neutron energy, E_{out}, range of the data, the affected part of the data will be rejected.
- Partial uncertainties should be provided for: counting statistics, corrections of various backgrounds, multiple scattering and attenuation corrections, detector efficiency and/or response, correction accounting for angular distribution of measured fission fragments[3],

[3] Prompt neutrons are assumed to be emitted from fully accelerated fission fragments. If fission fragments are detected

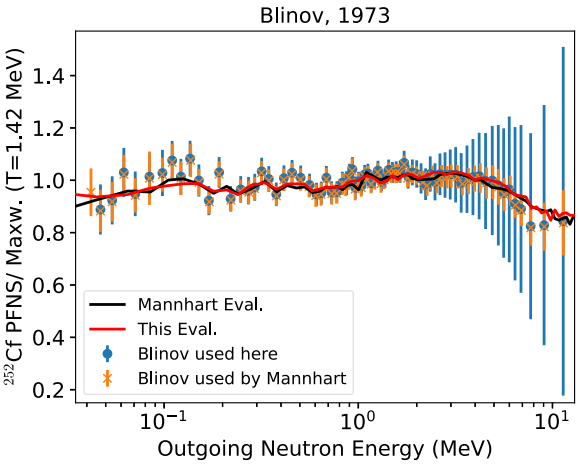

Fig. 1. Blinov, 1973 data read from Figures 5 and 6 of [11] compared to those used for the new evaluation based on EXFOR subentry 40418.007. Mannhart's and this evaluation are shown for comparison. Uncertainty bands of the evaluation are not given to increase readibility of the plot but are shown in Section 4.

deadtime corrections, uncertainties of nuclear data if used for simulations of measurement corrections, and impurities[4]. Also, l, Δl, and Δt should be provided.

- If partial uncertainties are not explicitly provided, but can be reasonably estimated based on existing total ones based on the journal article (e.g., by estimating the uncertainty based on the size of explicitly given correction factors), we will still accept a data set. Also, small missing experimental uncertainties will be estimated by templates of expected measurement uncertainties [47] if no other information is available.

3.2 Blinov et al. (1973) PFNS

Archival Details: The data by Blinov are described in Refs. [37–39] and in conference proceedings from 1973 and 1977 that are written in Russian language without translation. There are many subentries in EXFOR for the same measurement series. We identified subentry 40418.007 as the one that Mannhart used by comparing the measurement description and data points (Fig. 1[5]). The data in subentry 40418.002 could be superseded by the 40535 entries (see the next section). 40418.003 and 40418.004 are marked as preliminary, 40418.005 and 40418.006 are digitized from conference proceedings with little uncertainty information, while 40418.007 offers detailed uncertainty information. 40418.008 is a combination of measurement at three flight path lengths (25, 50, and 100 cm) which renders the analysis of time resolution inaccurate. We follow Mannhart's example and use 40418.007 as the data are final and detailed uncertainties are available. The metadata in Table 2 are given for this particular data set.

Experiment: Neutrons were measured using a ^{235}U fission chamber. A first stage of measurements was performed for 4 days indoors, while a second stage was undertaken outdoors, 9 m above floor scattering sources, for 21 days. The fission chamber efficiency was determined using a manganese bath along with Si detector measurements with 1° angular resolution. Measurements of the angular fission fragment-detection efficiency were made as well, to assess the effect of choosing specific neutron detector angles.

Results: All results were given relative to a 1.42 MeV Maxwellian. The ratio data are close to unity from 0.05–7 MeV, with a declining slope to ratio values near 0.8 at 10 MeV in Figure 1. The results display no features suggestive of issues in the detector response. Corrections were made for all effects listed above; highly detailed discussions are provided for each correction. Additionally, uncertainties were provided for counting statistics, the ^{235}U(n,f) cross sections, Δt, Δl, multiple scattering corrections (for scattering on air and structural material of detectors), background, random-coincidence background, for the anisotropy correction of the fission fragments and corrections of kinematic effects. Small deadtime and impurity uncertainties are taken from templates.

Potential Issues: None were noted.

3.3 Blinov et al. (1980) PFNS

Archival Details: The data by Blinov from EXFOR entry 40535 (first recorded reference in Russian language from 1980) are described in Ref. [50]. There are four subentries, each corresponding to a different flight-path length and energy range as listed in Table 2. None of the 40535 data were used by Mannhart. He neither cited them nor documented a reason why this particular data set was rejected. However, he rejected data if they were not corrected for "non-isotropic losses in the fission fragment detector" (termed angular distribution of fission fragments here) and "uncorrected stop signals in the electronic circuit" (termed random coincidences here) [22]. The former correction is not explicitly called out for this data set, but it was undertaken from the 1973 data set by the same group. Also, higher-energy boosted neutrons are the most impacted by angular fragment distribution losses, whereas this measurement is at low energies. Hence, even if the effect was not corrected, we assume it to be small.

Experiment: Neutrons were detected via a ^{6}Li(Eu) crystal. A gas scintillation counter detected fission fragments with two samples of ^{252}Cf (layers) over a measurement time of 110 days. The neutron detection response was calculated via MC simulations using ENDF/B-V.0 ^{6}Li(n,α)

with lower probability at specific angles, e.g., when fragments are lost for emission along the longest sample axes, this effect needs to be corrected.

[4] Sample impurities, such as from ^{249,250}Cf, should bias the experimental data only a little, because their PFNS shapes are expected to be similar [53].

[5] Low-energy data are shown on a logarithmic x axis to enhance visibility of low-energy points. High-energy data are shown on a linear scale to emphasize coverage at higher energies.

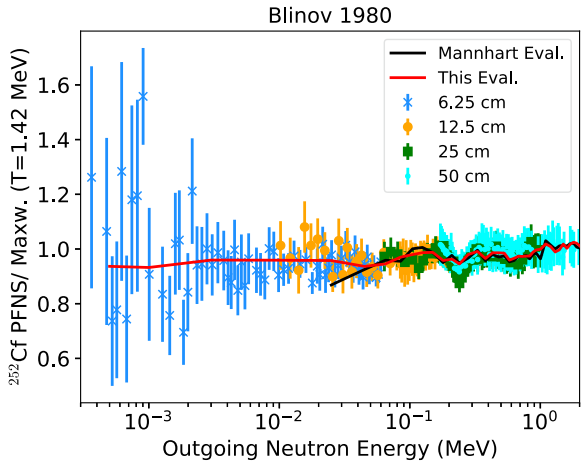

Fig. 2. Blinov, 1980 data measured at different flight-path lengths compared to Mannhart's and this evaluation.

cross sections [54]. The measurements were made for very low E_{out}, where backgrounds and multiple scattering lead to major correction factors. These effects were minimized by using neither shielding nor a shadow bar. Multiple scattering on air, walls, and the detector were MC simulated and measured (using a second detector with doubled mass), and relative corrections were supplied for the 6.25 cm measurement.

Results: The data in Figure 2 correspond well to Mannhart's evaluation from 50 keV to 2 MeV despite not being included. They are higher than the evaluation from 25–50 keV. Only Dyachenko et al. and Boldeman et al. data provided input for Mannhart's evaluation at this energy. However, the Dyachenko and Boldeman data sets show wave-like structures due to insufficient corrections of the ^{6}Li peak, while Blinov, 1980 data stay comparably flat relative to the assumed Mawellian of 1.42 MeV. Corrections were made for nearly all important effects; as mentioned above, it is not explicitly stated if the angular distribution of fission fragments was accounted for when calculating the fission-detector efficiency. The total uncertainties in EXFOR contain statistical and correction uncertainties – not accounting for the ENDF/B-V.0 monitor uncertainties that define the missing detector response uncertainties. Partial uncertainties for corrections were not provided but the correction factors are given. The associated uncertainties were estimated to be 10% of the correction. The γ background was no more than 0.5%, the random-coincidence background was 0.07% at 100 keV and 6% at 5 keV. Multiple-scattering corrections were 0.1% at 100 keV, 7% at 10 keV, and 2% at 1 keV. The contribution of impurities was determined to be negligible. Given the EXFOR total uncertainties and the assumptions above, statistical uncertainties were backed out and ENDF/B-V.0 monitor uncertainties were added. Energy uncertainties were explicitly given.

Potential Issues: While the effect is not correctly resolving the ^{6}Li peak is much smaller in Figure 2 for Blinov compared to Dyachenko et al. and Boldeman et al. data (Figs. 7 and 4), it is still causing a visible dip in that region. So, we removed some of the affected experimental data in that energy range for the evaluation.

3.4 Böttger et al. PFNS

Archival Details: The data by Böttger et al. are not yet in the EXFOR database. We used E_{out}, mean values and total uncertainties read from Figure 2 of [11], and information from Refs. [26–29] to obtain these data.

Experiment: The ^{252}Cf source for measurements carried out from 1981–1982 [27] and from 1985–1986 [26] both used a low-mass parallel-plate ionization chamber, but details of these sources such as the construction and activity were different for each data set. Differences of these chambers are described in Table I of Ref. [26]. Neutrons were detected with four large NE-213 scintillators in the same room. They stood approximately 2 m apart from neighboring scintillators. Exit collimators were placed between fission and neutron detectors. Each neutron detector was positioned behind massive neutron shielding at the exit of collimation holes. Neutron efficiency values were assessed using the NEFF and NRES [55] codes, and compared to monoenergetic response experiments using the NE-213 detectors that were calibrated with proton-recoil telescopes. The effect on the PFNS from changing angles for neutron detection was studied, and no individual correction was required for the neutron detectors.

Results: Results are shown separately for each detector combination in Ref. [26] and appear to agree well within uncertainties. We use Böttger data by Mannhart, who combined all measurement runs from 1981–1982 and 1985–1986 by weighting each with their statistical and systematic uncertainties. Relative to a 1.42 MeV Maxwellian, the data are near unity in the 2–6 MeV range in Figure 3, with a decline to a ratio of ≈0.75–0.85 at 14 MeV. This trend is consistent with most other measurements in this range, as well as the Mannhart evaluation itself. Only total uncertainties could be read from Figure 2 of Ref. [11], but extensive calculations and studies for sources of systematic errors and uncertainties were carried out for analysis of these data. Partial uncertainties are described [26,27,29] for the neutron and fission detector efficiencies, attenuation, multiple scattering, background, and counting statistics along with TOF resolution and TOF length uncertainties. Impurity and deadtime uncertainties were not provided and were therefore assumed from templates, but these uncertainties are small. The background uncertainties were only described approximately (2% at lowest E_{out} and then increasing), but could be backed out from total uncertainties.

Potential Issues: This measurement was exceptionally thorough; it provided an extensive list of uncertainties and potential sources of error. One concern is the potential for scattering between neutron detectors behind the heavy shielding. However, the neutron detectors are approximately 2 m apart, so that multiple scattering between

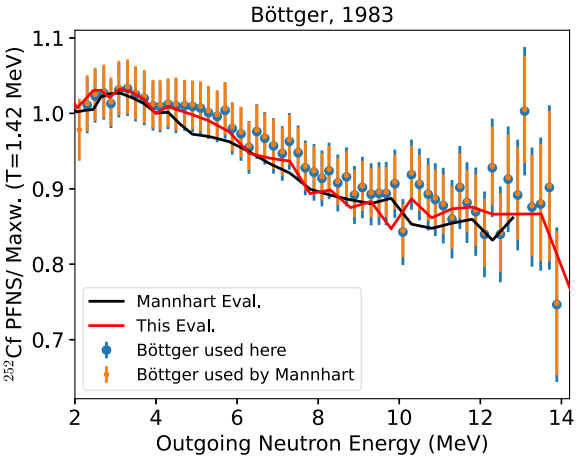

Fig. 3. Böttger, 1983 data read from Figure 2 of Ref. [11] compared with those used for the new evaluation. The two experimental data sets are nearly the same except for small differences in the uncertainties.

them is likely a smaller effect compared with neutron scattering from walls and floors. As data are provided at $E_{\text{out}} > 2$ MeV, these issues likely generate only a modest error in the results.

3.5 Boldeman et al. PFNS

Archival Details: The data by Boldeman et al. [40] appear in EXFOR subentries 30775.003 (^{6}Li-glass scintillator, $E_{\text{out}} < 3$ MeV) and 30775.002 (NE-102 plastic scintillator, $E_{\text{out}} > 1$ MeV). The mean values used by Mannhart agree with most EXFOR mean values in Figure 4. Mannhart rejected six data points around the ^{6}Li peak, the highest two data points of subentry 30775.003 and three unspecified data points of 30775.002. We reject ^{6}Li-glass data in their entirety, but accept plastic scintillator data.

Experiment: This work summarized eight experiments to measure the ^{252}Cf(sf) PFNS: seven measurements using a NE-102 plastic scintillator combined to form a single result for 1.05–14.25 MeV, and one measurement using a ^{6}Li-glass detector from 0.124–2.660 MeV. Fission events were measured with a methane-filled parallel-plate ionization chamber. The efficiency for fragment detection was measured with a Marion counter. No collimation was used between the fission and the neutron detector in order to avoid scattering off of the collimator itself. Measurements were made with a raised, 5 m high experiment area to minimize neutron scattering from the floor, with a 90 cm polyethylene shadow bar used for NE-102 measurements only to reduce the time-dependent background. The efficiency of the neutron detector in the 0.5–2.0 MeV energy region was determined relative to a long counter [56]. The long counter was calibrated using yields from $T(p,n)$ and ^{7}Li(p,n) source reactions rather than Neutron Data Standards.

Results: Corrections for detector dead time, air attenuation, delayed neutrons and γ rays, air-scattered neutrons, timing resolution, and fission fragment loss below threshold were included in the analysis, with a thorough discussion. The ^{6}Li-glass results show energy-dependent shape deviations from a 1.42 MeV Maxwellian in the left-hand side of Figure 4: The broad peak with a centroid of approximately 240 keV coincides with the ^{6}Li(n,t) cross section resonance and is followed by a distinct drop from 300–400 keV and a slow rise to near unity. Data in the right-hand side of Figure 4 from 1.0–5.0 MeV show a roughly flat ratio slightly above unity within statistics relative to the same Maxwellian, followed by a slow decline to a ratio of approximately 0.9 at 10 MeV. These features of the NE-102 data agree with other measurements in the same energy ranges. Data above 10 MeV vary between Maxwellian ratios of 0.754 and 1.072, but with large uncertainties. Unfortunately, no detailed partial uncertainties were provided. Statistical and total uncertainties are identical to the digit in EXFOR subentry 30775.003 and these uncertainty data are very similar in 30775.002, which is unrealistic. We assume a deadtime uncertainty equal to 10% of the deadtime correction, and other uncertainties (background, multiple scattering, detector efficiency uncertainty, etc.) using templates.

Potential Issues: The NE-102 scintillator efficiency was measured with the associated particle method at a Van de Graaff accelerator. There was no mention of keeping the experimental environment the same as in the PFNS measurement, though at high E_{out} this is likely not an issue. On the other hand, the Li-glass efficiency measurement, also measured at a Van de Graaff accelerator, was explicitly stated to be as close to identical to the PFNS measurement as possible including an effort to match the time resolution to the PFNS measurement. This statement likely reflects that an increased effect from neutron scattering was expected for lower E_{out} PFNS, as well as effects relating to scattering from the detector housing and PMT mentioned by the authors. While the response functions for neutron energies up to 1.4 MeV were measured with this method, the response to neutrons above this energy were approximated by assuming a similar shape as the lower-energy functions. These functions were subsequently utilized in an unfolding procedure to obtain the final results, but details of the unfolding method itself could not be determined. As noted above, Li-glass data also show suspicious features resembling the ^{6}Li(n,t) resonance near 240 keV and a sharp decline above this resonance. We note that the potential for scission neutrons was included by "folding" a 1.07 MeV Maxwellian into the results, though this likely did not create any major issues. The use of $T(p,n)$ and ^{7}Li(p,n) source reactions for determining the neutron-detection efficiency causes some concern as the data for the angular distribution yields were not documented. In addition, the setup is not discussed, but one does need to know solid angle subtended by the long counter from the neutron source. Furthermore, the ^{7}Li(p,n) yield data are not given and it is unclear what the weighting of the $T(p,n)$ versus the ^{7}Li(p,n) yields was. Lastly, there is a concern on the energy scale of the

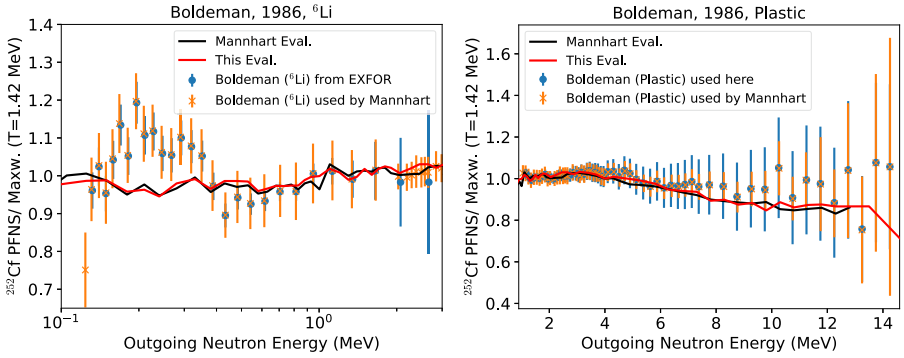

(a) (b)

Fig. 4. Boldeman, 1986 data read from Figures 7, 8 and 9 of [11] compared with those used for the new evaluation based on EXFOR subentries 30775.002/003. (a) Li scintillator. (b) NE-102 plastic scintillator.

^{6}Li data. Boldeman measured the energy scale via resonance positions using monoenergetic neutrons and found good agreement with Standards and accepted values. But, the spectrum measurement was done using TOF, potentially leading to an inconsistency. They noted this concern on p. 191 of Ref. [40] and measured the position of the 2.078 MeV ^{12}C elastic scattering resonance which achieved good agreement, but this was only done with the plastic scintillator and not with the ^{6}Li detector.

Despite valuable conversations with Boldeman himself, no firm conclusion could be made on the origin of the structure in the Boldeman data near the ^{6}Li(n,t) resonance feature at approximately 240 keV. The primary issue hindering definitive conclusions is that the unfolding routine utilized during analysis of these data could not be recovered and no documentation on the details of this method could be found. However, calculations of the ^{6}Li(n,t) reaction cross section convolved with a 1.42 MeV Maxwellian distribution folded with the energy binning of the Boldeman results were carried out with insights from Monte Carlo simulations of the response of ^{6}Li-glass detectors to the same Maxwellian function in order to investigate potential systematic errors in these data. These investigations suggested that the inclusion (or exclusion) of the neutron response above the maximum reported energy range of the ^{6}Li-glass Boldeman results may be partially or solely responsible for the presence of this structure in the data.

3.6 Boytsov et al. PFNS

Archival Details: There are several EXFOR subentries and publications related ^{252}Cf(sf) PFNS taken by the group of Boytsov, Nefedov, Starostov, et al., which can be a source of confusion. We reviewed EXFOR subentries 40871.005 (1st cycle, stilbene), 40872.002 (1st cycle, plastic), 40874.002 (1st cycle, anthracene), 40874.003 (2nd cycle, thin-wall ionization chamber), 40874.003 (2nd cycle, gas scintillation), and 40644.002. The last data set is marked as preliminary and will not be discussed here. All other data sets are shown in Figure 5. Mannhart rejected all these data sets stating only that they "did not pass quality criteria".

Experiment: The data were taken in two cycles: A miniaturized ionization chamber and gas scintillation detector were used for the 1st and 2nd cycle, respectively, to register fission fragments. For cycle 1, an anthracene detector was used to detect neutrons from 0.1–2 MeV, a stilbene scintillator (height of 3 cm and diameter of 7 cm, TOF path length: 231.3 cm) from 1.4–8 MeV and a plastic scintillator (height of 12 cm and diameter of 20 cm, TOF path length: 611 cm) from 3–12 MeV. In the second cycle, an ionization chamber and a gas scintillation ionization chamber were used. The neutron detector response was MC simulated with ^{1}H and ^{12}C nuclear data for the anthracene detector. ^{252}Cf(sf) PFNS data were used to derive efficiency values for the stilbene and plastic scintillator measurements, while ^{235}U(n,f) cross sections were used to determine the neutron-detector efficiency of measurements in the 2nd cycle.

Results: The authors assumed a Mawellian with T = 1.417 MeV for their data. Corrections were described for many effects listed above as required; it is unknown if deadtime, sample decay, transmission through the shadow cone for background determination, and α background were accounted for in the corrections. The data of the 2nd cycle and those measured with an anthracene detector agree remarkably well with Mannhart's evaluation in Figure 5 despite not being included in the evaluation. There are systematic discrepancies between Mannhart's evaluation and measured data using the stilbene and plastic scintillators above 3 MeV, where the data by the group of Boytsov et al. show trends to an increased PFNS compared to Mannhart's and this evaluation. Partial uncertainties are provided for most major effects including those due to counting statistics, background, multiple scattering, detector efficiency, and time resolution. TOF length uncertainties are also given and it is stated that corrections for angular distribution (and, hence, we assume the related uncertainties) are negligible. We assume small deadtime and impurity uncertainties from templates.

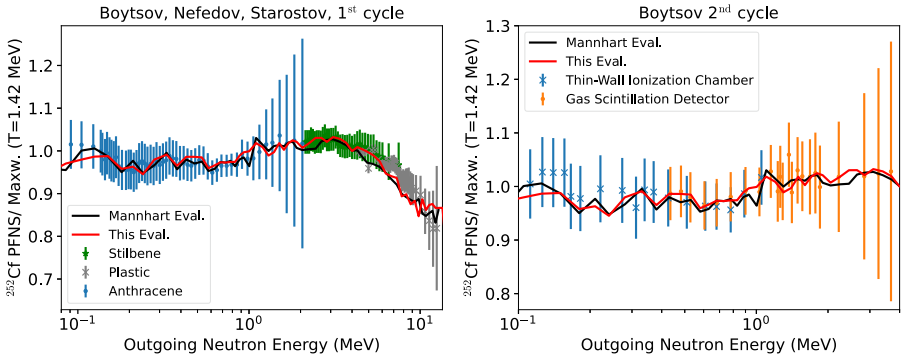

(a) (b)

Fig. 5. Boytsov et al., 1983 data measured in the 1st (left) and 2nd (right) experiment cycle with different detectors compared with Mannhart's and this evaluation. The data of the 2nd cycle and those measured with the anthracene detector are shown as used for the evaluation, while the data measured with stilbene and plastic scintillator detectors are shown as retrieved from EXFOR. (a) 1st cycle. (b) 2nd cycle.

Potential Issues: The data measured with the anthracene detector and those obtained in the 2nd cycle above 100 keV were accepted for the evaluation. We decided to reject data below 100 keV as the efficiencies were obtained relative to the ^{235}U(n,f) cross section. Below 100 keV, structures appear in this cross section due to unresolved resonances that are not accounted for in nuclear data and, hence, bias the resulting experimental data. The data measured with the stilbene and plastic scintillator had to be rejected as a ^{252}Cf(sf) PFNS was assumed to derive the detector efficiency, which is a circular argument and biases the experimental data towards the assumed PFNS.

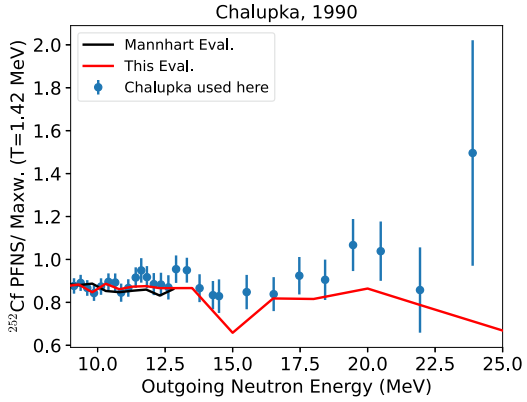

Fig. 6. Chalupka, 1990 data used here compared with Mannhart's and this evaluation.

3.7 Chalupka et al. PFNS

Archival Details: The data by Chalupka et al. [15] are in EXFOR subentries 22202.003 (9–12.76 MeV), 22202.004 (13.98–27.10 MeV), 22202.005 (9–15.52 MeV), 22202.006 (9–18.94 MeV), and 22202.007 (9.99–20.02 MeV). The different EXFOR entries correspond to different energy ranges or bias settings (2 and 2.75 MeV). They can be combined considering correlations if different energies are used; otherwise, one would double count data as they stem from the same raw data. We used part of data from subentries 003, 004, and 005 shown in Figure 6 for the evaluation. The journal publications were published after Mannhart's evaluation in Ref. [11]. Mannhart included Chalupka data in a subsequent evaluation, documented in Ref. [21]. However, and this is puzzling, this newer evaluation of Ref. [21] was not released to the Standards but rather the older one of Ref. [11]. To add further confusion, in 2008, Mannhart recommended including Chalupka et al. data along with those of Märten et al. for future evaluations [57].

Experiment: The main aim of this measurement was to counter-check the upturn of the PFNS above 20 MeV seen by the Märten et al. group [33] which was contrary to the evaluation by Mannhart. They identify background from cosmic radiation as main potential issue above 20 MeV in that measurement. In order to reduce this specific background, Chalupka et al. performed their measurement in a mine in Bad Bleiberg, Austria which is 1000 m below a mountain known as a rich harvesting grounds for lead and tin. In essence, the mountain served as a 1000 m thick natural Pb shield to reduce random-coincidence background triggered by cosmic radiation. One NE-213 scintillation detector was used for all runs to count neutrons. Its efficiency values were MC calculated using NEFF-4 [55] up to 20 MeV. For 18–29 MeV, Chalupka et al. used the ^{1}H cross sections adjusted to NEFF results between 16–18 MeV, which agree well with today's JENDL-5.0 data. The light output curves were calibrated with ^{22}Na, ^{60}Co, and ^{208}Tl Compton edge energies. Fission fragments were detected in an 99.5% efficient fission chamber. Given the description, it is possible that the detectors used were those also employed by Böttger et al. [28].

Results: Corrections were made for all known effects, and detailed partial uncertainties were provided for all uncertainties explicitly, or it was stated that they were 0. The measured data meander around Mannhart's evaluation up

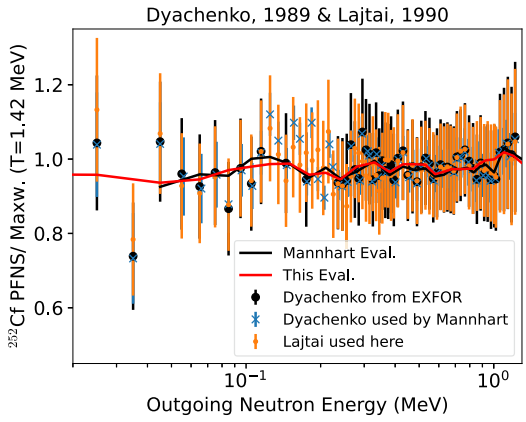

Fig. 7. Dyachenko, 1989 read from Figure 1 of [11] compared with EXFOR data by the same author and Lajtai, 1990 data used for the new evaluation presented here.

to 12.5 MeV in Figure 6, and then show, within uncertainties, a trend similar to a Maxwellian with temperature of 1.42 MeV until 22.5 MeV. These data do also show a slight oscillatory pattern relative to Mannhart's evaluation, but these fluctuations are generally small and within 1–2σ of the reported results.

Potential Issues: There were two minor concerns: One was that the carbon cross sections used in NEFF-4 agreed with JENDL-5.0 only to 7% (total) and 9% (inelastic); however, their influence should be small as the main cross section used is ^{1}H. Also, it was not completely clear in how far the ^{252}Cf(sf) PFNS was used for the detector response. Unfortunately, the authors of this data set could not clarify this. As these are minor concerns, and many important corrections were performed and detailed uncertainties are provided, we accept the data until 22 MeV removing one outlier around 25 MeV.

3.8 Dyachenko et al. and Lajtai et al. PFNS

Archival Details: The data by Dyachenko et al. are in EXFOR subentries 40875.003 (data as ratio to Maxwellian) and 40875.002 (shape data, neutron-detector efficiency, energy-dependent uncertainties for neutron-detector efficiency and response-function correction). The data were published as a journal article and proceeding [24,25]. What Mannhart terms "Lajtai data" in Ref. [11] are actually Dyachenko data; the data read from Figure 1 of [11] are nearly the same as in EXFOR (see Fig. 7). The data by Lajtai et al. are in EXFOR subentries 41158.003 (data as ratio to Maxwellian) and 41158.002 (shape data, neutron-detector efficiencies and their energy-dependent uncertainties). They supersede Dyachenko data [14]. Both data sets stem from the same raw data, and, most features and analysis techniques are the same. So, they are described in one section.

Experiment: Both data sets used an NE-912 ^{6}Li-glass detector to count neutrons. The neutron-detector efficiency is explicitly given in Table 1 of Ref. [24]; it was simulated via the MC code BRAND by P.A. Androsenko and A.A. Androsenko for a 0.0835 cm thin ^{6}Li-glass detector (NE-908). The efficiency for the NE-912 detector was derived by a relative measurement to the NE-908 measurement. The NE-912 detector was not directly simulated to avoid limitations in accurately computing multiple scattering and attenuation.

More recent MCNP simulations [58] for Lajtai data verified the efficiencies for most energies except for 200 keV (the ^{6}Li peak) for the NE-912 detector. There, Lajtai's efficiency is more than 10% higher. While both simulations have limitations (missing environmental effects), it is interesting to note that Lajtai data show an increase at these energies that is not observed by Poenitz. An NE-913 ^{7}Li detector (only sensitive to γ rays) of the same size as of the NE-912 detector was used to measured background from delayed γ rays. All other backgrounds were obtained by measuring with and without a brass shadow cone. Fission fragments were detected in a fission chamber using thin-film ^{252}Cf deposits.

Results: The two data sets differ in the simulations of neutron efficiencies: according to Ref. [49], errors were found in the MC simulations of the neutron detection efficiencies of [24,25] that are corrected in Ref. [14]. The correction leads to distinct differences between Dyachenko and Lajtai data from 150–350 keV in Figure 7 where the ^{6}Li(n,t) cross section resonance is situated. Incorrect neutron efficiencies would be enhanced through that strong structure in that cross section and lead to features in ^{252}Cf(sf) PFNS that are more evident in Dyachenko data (sharp up and down of data compared to a Maxwellian), while Lajtai data exhibit a more flat behavior. Corrections were undertaken for many major effects except for the anisotropy of fission fragment emission, the shadow-bar background, and neutron attenuation and multiple scattering in the sample. Total uncertainties provided in EXFOR contain statistical uncertainties (foreground and background), uncertainties in the detector-response calculation (2%), in the neutron-detection efficiency (given explicitly), the fission-detection efficiency (3%), the TOF length (1 mm), and the solid angle (2%). Only deadtime uncertainties needed to be assumed from templates.

Potential Issues: One major concern is how the brass shadow bar was used. It was situated between the fission and neutron detector without shielding. This approach could cause substantial additional environmental neutron scattering that was not well matched by the background measurement. However, the authors assumed the shadow cone to be a perfect absorber for neutrons emitted from the fission chamber. It was shown in Ref. [58] that this is not the case, resulting in an estimated error on the PFNS of 10% which we take as additional uncertainty. Another issue is that the detector response was only simulated including the material of the crystal and not the environmental surrounding materials. Lastly, Figures 2 and 3 of Ref. [24] and Figure 2 of Ref. [14] show a smearing of the detector response to higher energies; only a smearing to lower energies is expected. Mistakes in the response function could have an especially pronounced effect on PFNS values above the ^{6}Li resonance.

3.9 Kornilov PFNS

Archival Details: The data by Kornilov [12] are in EXFOR subentries 14431.002 and were published after Mannhart's evaluation as an INDC report.

Experiment: The experimental data were taken in 4500 h over 4 years. Kornilov accounted for the decay of the sample and measured also the detector's stability to mitigate any potential adverse effects due to the long measurement time. The data reported in EXFOR are from a combination of runs 3, 5, and 7 that used the same sample. In Dec. 2009, the sample make-up was in mass-percentage 45.674% ^{252}Cf, 14.602% ^{251}Cf, 30.082% ^{250}Cf and 9.641% ^{249}Cf, while it was in April 2012 for run 7 (latest measurement and thus "worst case"), 32.92%, 18.76%, 35.49% and 12.83%, respectively. Still, approximately 99.4% of all fission were from ^{252}Cf for run 7. Neutrons were counted with one scintillation detector of type NE-213 for these runs. The efficiency values of the neutron detector were calculated by the MC technique using GEANT4 and NEFF-7 [59,60] leveraging the dynamic threshold method to go up to 20 MeV. The light output of the detector was measured with a white neutron source until 12 MeV. From a schematic drawing, it appears that the neutron detector was located at 0° relative to the normal to the plane of the ^{252}Cf deposit. Fission fragments were detected in an ionization chamber. Neutron data taken in coincidence with the ^{252}Cf chamber were normalized to the Mannhart's evaluation to correct for the constant part of fission events below the threshold.

Results: Kornilov data in the left-hand side of Figure 8 are within uncertainties of Mannhart's evaluation until 12.5 MeV. Then the data are trending towards a value of 0.5 in ratio to a 1.42 MeV Maxwellian with a peculiar structure close to 20 MeV. These characteristics, along with unusual structure below 5 MeV, were highlighted by the machine-learning analysis in Ref. [61] as indicative of biases in the data. These findings motivated additional investigations presented below. An increase of the PFNS is also observed in Chalupka data (right-hand side of Fig. 8) close to 20 MeV but is distinctly weaker than the Kornilov data (value of approximately 1.1 for Chalupka versus 1.5 for Kornilov data at 15 MeV). Corrections were documented in Ref. [12] for γ-ray background, neutron multiple scattering and attenuation in the sample and surrounding, decay of the sample, neutron-detection efficiency, fission-detector efficiency (including anisotropy of fragment emission and absorption in the sample) and deadtime. The nature of uncertainties provided in EXFOR is not specified. The article states that the deviation of experimental data from evaluated ^{252}Cf(sf) PFNS by Mannhart could be seen as the systematic uncertainty of the dynamic threshold method (3% below 3 MeV, 2.0% for 2–7 MeV, 2.5% from 7–10 MeV, and 4.0% for 10–13 MeV). The TOF length uncertainty is given with 5 mm.

Potential Issues:

- The following uncertainty sources are missing: counting statistics, background, Δt, multiple scattering, deadtime, impurity and anisotropy of fission fragments.
- It was unclear if random coincidences (could bias results above 10–12 MeV) and α background were corrected, and how good the γ-neutron separation was. Unfortunately, Ref. [12] does not provide a two-dimensional figure that shows the quality of γ-neutron separation which could be a major source of bias.
- Another issue is that the simulation to account for multiple scattering and the detector response is incomplete as only a simplified model of the detector was used for the MC simulation (Fig. 17 in [12]), and it seems that collimators were not considered for this simulation.
- The light curve was extrapolated above 12 MeV. A small mistake in this extrapolation could have large impacts on the detector response.

Revision of data: At the time of the revision of Kornilov's data, the author was unfortunately deceased. However, key information could be retrieved from his work computer enabling this revision. This information includes that the flight path length for relevant runs was 4.238 m, Δt was likely approximately 2.4 ns (FWHM), and more realistic TOF length uncertainties of 2.5 cm. Also, the PFNS data for runs 3, 5, and 7 were found along with their statistical uncertainties. We statistically combined data from only runs 5 and 7 and termed these new data "Reanalyzed Kornilov" data in Figure 8. Run 3 was rejected as its light output parameters and linearity were inconsistent with runs 5 and 7 (Table 3 and Fig. 14 in Ref. [12]) leading to systematically different data below 4.5 and above 15 MeV in Figure 9.

Also, the raw data could be reanalyzed and two-dimensional PSD plots could be reproduced that showed very good γ neutron separation. While the original report does not call out random coincidences as being corrected, the procedure for this correction was described by Kornilov in Ref. [62] and was in fact applied to the data set here as a standard procedure of the group. This correction will also have implicitly corrected the α background. Based on this additional information, we estimated the remaining background uncertainty to be 3% until 10 MeV, and 10% above. Deadtime, impurity, and angular distribution uncertainties are assumed to be negligibly small. Drawings from the experiment set-up would indicate that (multiple) scattering from the collimators, an effect that was not accounted for in the MC simulations, could be assumed small, and the simplified MC simulations to be a reasonable approximation. Still, we assumed multiple scattering uncertainties linearly rising from 0.5% to 3% from 2–10 MeV, and then constant with 3% above.

One remaining concern was the extrapolation of the light curve and resulting potential mistakes in the detector efficiency which could lead to the erratic behavior in the data observed at high and low energies in Figure 9. As incorrect light curves could impact the PFNS at low and high energies, we decided to reject data below 4.4 and above 13.4 MeV where the different runs were showing different behavior. Also, Kornilov data vary distinctly above 13.4 MeV within themselves compared to other data sets.

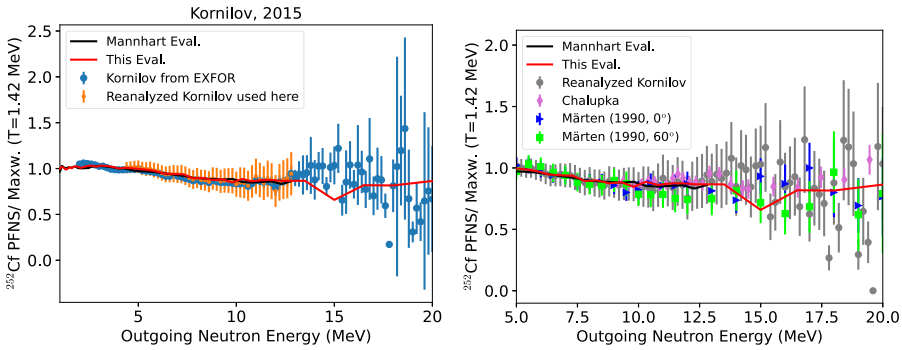

Fig. 8. (Left) Kornilov, 2015 data used here and from EXFOR compared with Mannhart's and this evaluation. (Right) Reanalyzed Kornilov data are compared to those of Märten (1990) and Chalupka above 5 MeV.

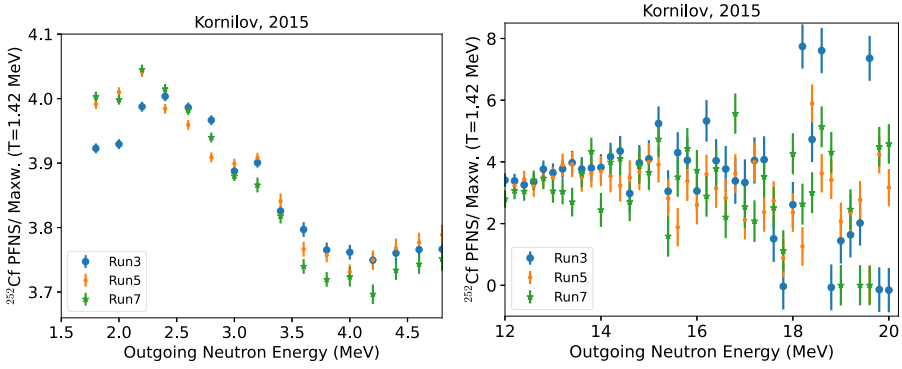

Fig. 9. Data from runs 3, 5 and 7 of Kornilov are compared from 1.5–4.5 (left) and 12–20 (right) MeV.

3.10 Märten et al. (1984) PFNS

Archival Details: The data by Märten et al. are in EXFOR subentries 31854.002 (<20 MeV with detailed partial uncertainties) and 31854.003 (>20 MeV and 75% interval). The data were published as laboratory reports and one proceeding [30–34]. They were only recently cast into EXFOR entries. However, these are not the same data as read from Figure 10 of Mannhart's conference proceeding [11] as can be seen in Figure 10. Mannhart explicitly stated that he only used data below 20 MeV, but even EXFOR data of subentry 31854.002 have slightly different shapes in the overlap region. So, we assume that Mannhart's data were obtained via private communication.

Experiment: Märten et al. used a highly-shielded NE-213 liquid scintillator to detect neutrons. The efficiency of this detector up to 15 MeV was calculated using the Stanton MC code [63] with Verbinski's light-output tables [64]; above 15 MeV, the efficiency values were extrapolated. This efficiency was validated by comparisons with the NBS evaluation of the ^{252}Cf(sf) PFNS [65] using an iterative method to reproduce this evaluation. Neutrons from the PFNS were identified using PSD and n-γ kinematics, which also removed part of the backgrounds from α particles and other sources of random coincidences. Fission fragments were detected in a fission chamber. The start signal for the TOF was initiated by neutrons measured in the NE-213 scintillator, and the stop signal was defined by a delayed fragment detection in the fission chamber. Data were collected over 1218.5 h of total experiment time.

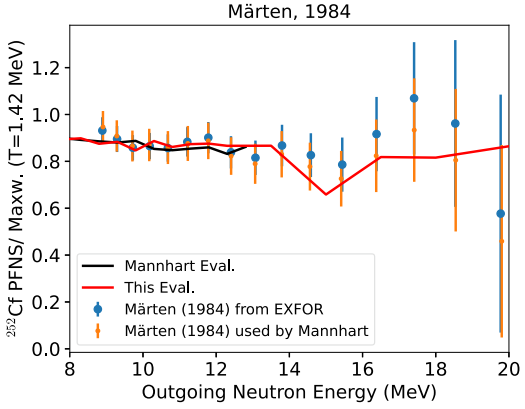

Fig. 10. Mäerten, 1984 read from Figure 10 of [11] compared with those studied here and found in EXFOR subentry 31854.002.

Results: The fitted Maxwellian to these data had a temperature of 1.374 MeV. Corrections were applied for nearly all effects mentioned above; it is only unknown if the decay of the sample was corrected for. Additionally, the following

corrections are listed in the EXFOR entry: γ peak correction (negligible), neutron transmission correction, TOF channel dependent background due to non-correlated stop signals (negligible), unfolding correction due to time resolution, bin-width correction, and fragment-detection efficiency. Partial uncertainties are provided in EXFOR subentry 31854.002 based on Table 2 of Ref. [30] for the following effects and uncertainty sources: statistical uncertainties, bin-width correction, energy scale, unfolding correction due to time resolution, multiple-scattering correction, light-output bias, and neutron-detector efficiency. Impurity uncertainties were not provided, and were assumed from templates, which are small.

Potential Issues: One major concern is that the neutron-detector efficiency was derived in a circular fashion by using the NBS ^{252}Cf(sf) spectrum as input for validating the detector response – the very same observable as measured. Thus, it is not surprising that the measured data correspond to the evaluated data. Another concern is that the calculation of the efficiency depends on the hydrogen and carbon cross sections, and that the latter ones have changed significantly above 15 MeV since the time of this measurement. The data above 20 MeV had sizable random-coincidence backgrounds that were not adequately accounted for when correcting the muon background. The data set was rejected for the new Standards evaluation, and is superseded by the data by the same group published 1990 in a journal article [13]. These new data did not rely on assuming a ^{252}Cf(sf) PFNS to derive the detector response.

3.11 Märten et al. (1990) PFNS

Archival Details: The data by Märten et al. in Figure 11 are in EXFOR subentry 30969.002 (measured at 0°) and 30969.003 (measured at 60°). They were published as a journal publication [13] contrary to EXFOR subentries 31854.002 and 31854.003 by the same group published as laboratory reports and proceedings. The 30969 data were finalized after Mannhart's evaluation. Similar to Chalupka et al. data, Mannhart used them for a later evaluation [21] that was not delivered to the Standards. In 2008, he recommended to take Märten et al. (1990) PFNS into account for future evaluations [57] which is puzzling.

Experiment: Märten et al. recorded neutron spectra as a function of TOF and scintillator pulse height. The use of PSD corrected for part of the background (from α contamination, γ ray backgrounds, and random coincidences). The team used two NE-213 neutron detectors at two different angles and TOF paths: (a) A 12.7 cm thick and 12.7 cm diameter scintillator was used at 0° with a TOF path length of 5.905 m and a time resolution of 1.5 ns. (b) A 3.81 cm thick and 12.7 cm diameter scintillator was used at 60° with a TOF path length of 3.275 m and a time resolution of 1.3 ns. The 60° measurement is strongly correlated with the 0° measurement. The neutron-detector efficiency (undocumented) was simulated via a MC code by Stanton [63] using light output curves by Cecil [66].

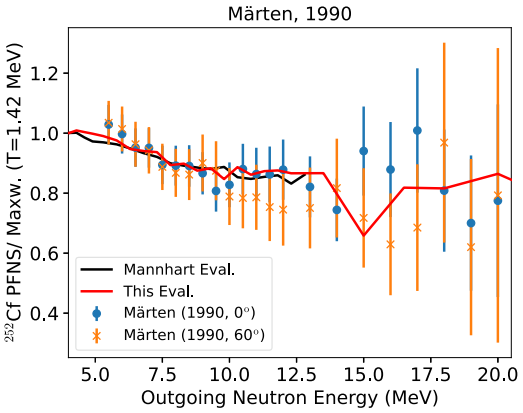

Fig. 11. Märten, 1990 data used here (0° data are shown with full circles, 60° data with crosses) compared with Mannhart's and this evaluation.

The authors carefully adjusted the simulation to consider the detector signal resolution (light output in terms of proton recoil equivalent). Also, they absolutely calibrated neutron-detection efficiencies of both detectors against their response from 14 MeV neutrons from a D+T neutron generator. The neutron source strength has been determined by counting the associated α particles produced in the D+T reaction (solid state detector positioned at a fixed backward angle) [67]. The detector response accounts for multiple scattering and attenuation in air, the surrounding, and detector walls. Fission fragments were detected as stop signal (delayed by 200 ns) in a miniaturized fission chamber.

Results: It is interesting to note that the data measured at two different angles in Figure 11 differ distinctly. This discrepancy was highlighted and related to angular dependency in the machine-learning bias model analysis in Ref. [61]. In fact, the main difference between these two data sets is the angle. Taking this information into account might call into question the treatment of the angular dependence of the fragment-detection efficiency inherent to the fission detectors despite the fact that it should be of 99.2% efficiency. The fitted Maxwellian to these data had a temperature of 1.374 MeV. Corrections were applied for nearly all desired effects mentioned above; it is only unknown if the decay of the sample was corrected. Additionally, the following corrections are listed in the journal article: γ peak correction (negligible), TOF channel dependent background due to non-correlated stop signals (negligible), unfolding correction due to time resolution, bin-width correction, and fragment-detection efficiency. Statistical and systematic uncertainties are provided in the EXFOR entry 30969.003 based on Table III of Ref. [13]. The systematic uncertainties contain uncertainties of the neutron-detection efficiency, energy scale, energy bin width, light-output calibration, and all corrections. Reference [13] cites to Ref. [30] for some partial uncertainties. Hence, we take partial uncertainties from EXFOR subentry 31854.002 for the bin-width correction, energy scale, unfolding correction due to time

resolution, multiple-scattering correction, light-output bias, and neutron-detector efficiency, and back out the remaining systematic uncertainties. Impurity uncertainties were not provided, and were assumed from templates, but are small.

Potential Issues: One major concern of entry 31854.002 (previous data [30]) was that the neutron-detector efficiency was derived in a circular fashion by using the NBS ^{252}Cf(sf) spectrum as input for validating the detector response. This issue was corrected by the authors in Ref. [13] by undertaking measurements of the detector response with a D+T generator that was also measured with the associated particle technique [67]. One open question is the strong discrepancy between PFNS at 0 versus 60° in Figure 11. Märten wrote in Ref. [13] that the spectrum at 60° is least distorted by anisotropic losses of fission fragments compared to 0 and 90°. Also, Chalupka notes in Ref. [68] that the fission fragment efficiency shows the least variation with neutron energy at 60°. The same effect was also observed and validated through the detailed analysis of data from the Chi-Nu ^{239}Pu(n,f) neutron-induced PFNS [69,70] (specifically, see Fig. 5 of Ref. [69]). It was determined in the latter work that the PFNS result integrated over a wide range of angles was largely insensitive to fission fragment detection efficiency effects, and that that differential result obtained at 60° and 120° were approximately equal to the integrated result. Monte Carlo simulations employing a known input spectrum confirmed these conclusions. Due to the above arguments, we accept the data measured at 60° and reject those at 0°. We also reject data above 20 MeV from [13]; the data rely on extrapolating the detector response beyond the D+T measurement and on simulations using carbon cross sections that changed significantly above 15 MeV since the time of this measurement. Not surprisingly, the data above 20 MeV show an unexpected upturn. Given that and the thoughtful consideration of all necessary corrections, we accept data set 30969.003 [13] (60°) for the new Standards evaluation and reject the previous data [30].

3.12 Poenitz and Tamura PFNS

Archival Details: The data by Poenitz and Tamura [35, 36] in EXFOR subentries 14278.002 and 14278.003, are close to those read from Figures 3 and 4 of Mannhart's conference proceeding [11] as can be seen in Figure 12. The main paper [35] is a conference proceeding and the data were marked as "preliminary"; no follow-up measurement was found.

Experiment: Poenitz and Tamura used two different "black" neutron detectors – scintillators of type NE-213 [36]. The smaller of the two was used from 0.2–4 MeV and the larger for 0.7–10 MeV. The efficiency values of both neutron detectors were calculated by the MC technique and experimentally verified with the associated-particle technique. Fission fragments were detected in a gas-scintillation counter.

Results: Most of the required corrections were accounted for. Uncertainties provided in EXFOR are total only

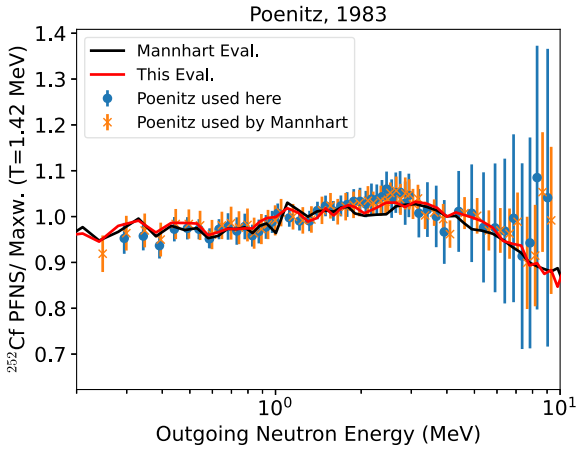

Fig. 12. Poenitz and Tamura data read from Figures 3 and 4 of [11] compared with those used for the new evaluation based on EXFOR subentry 14278.002.

– likely because the data were considered to be preliminary. However, Refs. [35,36] offer more information about uncertainties and corrections; the following effects were estimated to be negligible: ^{252}Cf migrating in the chamber (4.0×10^{-3}%), transmission from the shadow-bar (<0.1%), neutrons inscattering from the main collimator (<0.1%), neutrons inscattering from the first shield collimator (<0.2%), neutron scattering in the the sample, delayed γ and α backgrounds. The measured and simulated neutron detector response agreed within <1.2% for 0.5–0.9 MeV and 0.7% at 14.1 MeV, which one could take as a crude estimate for associated uncertainties. The TOF length uncertainty was 0.5–1 mm with a fitted Maxwellian of 1.439 MeV. A part of the background uncertainties can be gleaned from information on the fission-detector efficiency, namely, that 20 ± 2% losses in efficiency are due to α pile-up and 9 ± 3% due to total fragment absorption loss on fission-detector efficiency. The total uncertainties in Figure 12 estimated here are larger than those used for Mannhart's evaluation. The large uncertainties at high energies are driven by Δt which is large with 4 ns. It cannot be counter-checked if the same Δt value was considered in Mannhart's uncertainty estimate.

Potential Issues: Concerns were raised about the amount of shielding, and the shadow bar in the measurement. But the corrections were done well. The assembly was well-contained (closed environment), and the corrections should not pose an issue. There might be a small-angle effect of the collimator but it is very unlikely for that to happen.

4 Results

4.1 Reproducing Mannhart's evaluation

The left-hand side of Figure 13 shows that we were able to reproduce Mannhart's evaluated mean values for most energies within the 1-σ evaluated uncertainties

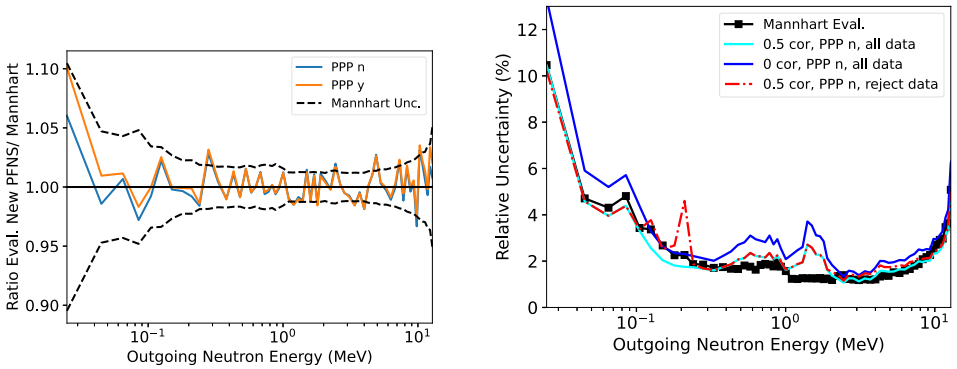

Fig. 13. (Left) Ratio of mean values of re-analysis of Mannhart's evaluation to the original one with ("PPP y") and without correcting the PPP effect ("PPP n"). (Right) Comparison of Mannhart's evaluated uncertainties to re-analyzed evaluated uncertainties under different assumptions of rejected data points and experimental correlation coefficients. (a) Comparison of mean values. (b) Comparison of relative uncertainties.

of Mannhart. We compare here to the pointwise, non-smoothed evaluation coming directly out of Mannhart's evaluation. The only point-wise evaluation that could be found spans an energy range of 25 keV to 12.8 MeV, while pointwise evaluated data up to 20 MeV are plotted in Ref. [11]. Differences to Mannhart' evaluation can be as low as 0.04% at 4 MeV and as high as 6% at the lowest energy point but generally are in the range of 0.3–3%.

Correcting the PPP effect with IRLS (PPP y in Fig. 13) leads to a slight increase of the evaluated PFNS in the wings. The effect ranges from 3.7–1.1% for 25–85 keV and from 1.6–1.3% above 11.8 MeV. Otherwise, the change in the PFNS is for many energies distinctly below 1%. Hence, neglecting to correct the PPP effect would have introduced only a small bias in Mannhart's evaluation.

We had to iterate through several different assumptions on the input data given that there are several aspects of Mannhart's evaluation that remain unknown according to Table 1. The impact of some of these assumptions on the evaluated uncertainties is shown in the right-hand side of Figure 13. One of the assumptions that had to be made is the average correlation coefficient between PFNS of the same experiment. If zero correlation for all off-diagonal covariances was chosen, the evaluated uncertainties would be noticeably larger than those of Mannhart. On the contrary, a correlation coefficient of 0.5 for each experimental covariance matrix reproduces Mannhart's evaluated uncertainties more closely. It is conceivable that the covariances for each experiment had complicated correlation shapes governed by their mixture of correlation shapes of individual uncertainty sources. As we do not know what the individual uncertainty sources were for each experiment that went into Mannhart's uncertainty quantification, guessing the resulting correlation structure remains futile. The impact of our average assumption being incorrect can be most clearly seen around 1–2 MeV, where the evaluated uncertainties using a correlation coefficient of 0.5 is distinctly higher than those of Mannhart. Here, the data of Dyachenko and Boldeman measured with a ^{6}Li detector would likely have had stronger correlations than 0.5 as the time resolution uncertainty would have dominated there. These stronger correlations would have pulled down the evaluated uncertainties to be in line with Mannhart.

A very isolated but strong deviation from Mannhart's evaluated uncertainties can be observed from 150–250 keV. Around this energy range, Mannhart noted in Ref. [11] that he rejected 9 data points by Dyachenko (from 125–305 keV) and 6 data points of Boldeman ^{6}Li data ("around the Li peak"). There are many more data points of Dyachenko and Boldeman in this energy range, so it remains guess work which ones exactly Mannhart rejected. After several trial-and-error versions of the evaluation with different rejected data points, the one shown in Figure 13 (left) led to good agreement with Mannhart's evaluated mean values, but the sharp deviation in evaluated uncertainties (right) indicates that we likely did not correctly identify all those experimental data points rejected by Mannhart.

In summary, while we are able to get reasonably close to Mannhart's evaluation, there are some aspects of his evaluation that will remain unknown. This limited knowledge renders it impossible to perfectly reproduce Mannhart's evaluation. However, getting as close as we do to Mannhart's evaluation indicates that our evaluation approach leads to defensible results.

4.2 New evaluation

The new evaluation is shown in Figures 1–8, 10–12 and 14. Here, we distinguish between the "pointwise evaluation" (shown in all plots mentioned before) and the "smoothed evaluation" (only shown in the left-hand side of Fig. 14) that is required for applications. The pointwise evaluation corresponds to results output by the GLS algorithm. The smoothed evaluation here was obtained by applying the Savitzky-Golay filter [71] using the `savgol_filter` function from the python package `scipy.signal` [72] with window length of 19 energy points and up to a

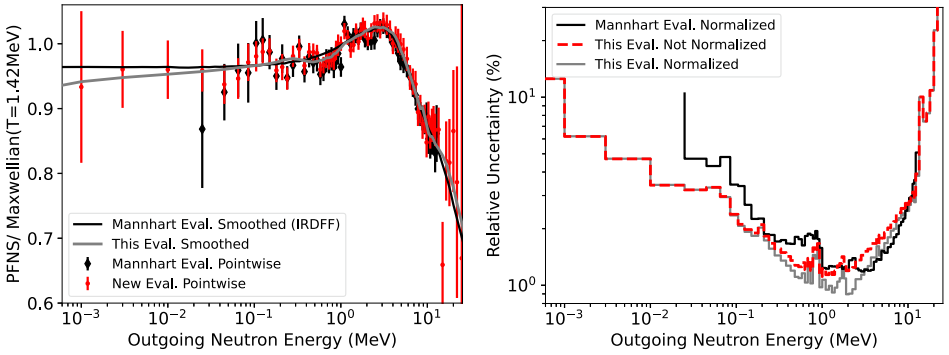

(a) (b)

Fig. 14. (Left) This evaluation (smoothed and pointwise) compared to Mannhart's (smoothed and pointwise). (Right) Comparison of Mannhart's evaluated uncertainties to evaluated uncertainties here. (a) Comparison of mean values. (b) Comparison of relative uncertainties.

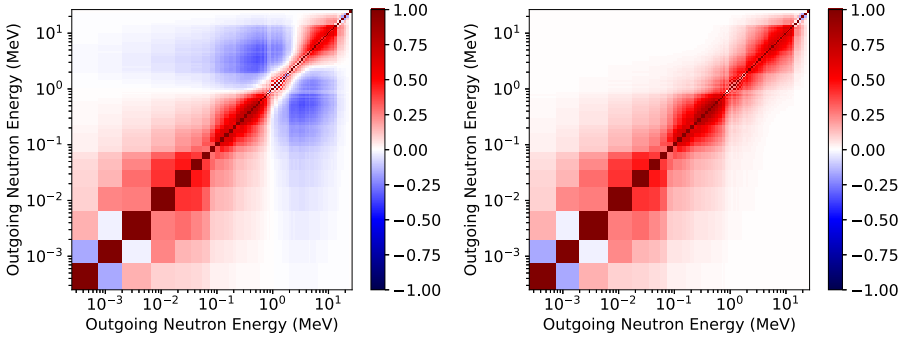

(a) (b)

Fig. 15. Evaluated correlations matrix after (left) and before (right) enforcing normalization on the evaluated PFNS. (a) Normalized. (b) Not normalized.

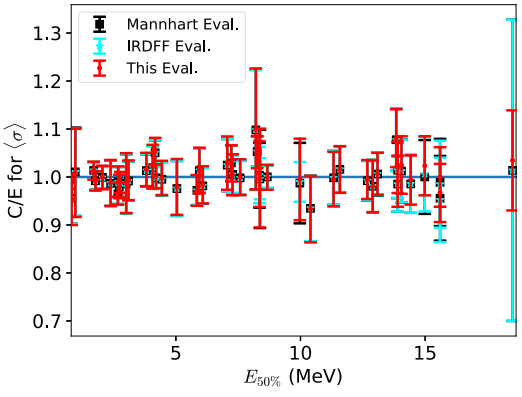

Fig. 16. C/E ratios of SACS, $\langle\sigma\rangle$, calculated with Mannhart's versus this evaluations to experimental data are compared to values from Table 18 in [48].

third polynomial order to the pointwise data that were divided through a Maxwellian with $T = 1.42$ MeV. Then, a Maxwellian was fitted to the first and last three data points separetly ($T = \{1.492, 1.391\}$, respectively) to extrapolate down to 1×10^{-5} eV and up to 30 MeV. The smoothed version of Mannhart's evaluation was retrieved from the IRDFF database [48].

The pointwise, new evaluation in Figure 14 covers a larger energy range compared to Mannhart's evaluation. The new evaluation starts at 0.5 keV (rather than 25 keV for Mannhart's pointwise evaluation) as it considers the Blinov et al., 1980 PFNS data that reach these low energies. The new evaluation follows the overall trend of these data within their uncertainties in Figure 2 except for three outlying experimental data points. The new evaluation could be extended up to 30 MeV because of including Chalupka et al. and Märten et al., 1990 (60°) PFNS data. At 15 MeV, one evaluated point is significantly lower than the trend of neighboring points. This evaluated point follows the trend by Märten et al., 1990 (60°) and Böttger et al. PFNS data close to 15 MeV but is contrary to trends in Chalupka et al. and Boldeman et al., plastic data. The smoothed evaluation removes this unphysical structure likely caused by statistical fluctuations in Märten et al., 1990 (60°) and Böttger et al. PFNS.

This and Mannhart's pointwise evaluation are close above 2 MeV, but the former has less structures close to the energy range of the ^{6}Li peak. There are fewer structures in the evaluated PFNS from 25 keV–1 MeV compared to Mannhart's evaluation as we reject Boldeman,

Table 4. SACS in a ^{252}Cf(sf) neutron field, $\langle\sigma\rangle$, are tabulated for various dosimetry reactions. SACS were either calculated with Mannhart's PFNS or this evaluation (AIACHNE). Also, experimental data are shown as retrieved from Table 18 in [48] and selected high-energy SACS measured in Řež retrieved from Table 19 in [48] (with bold reaction ID). The variable δ denotes the relative uncertainty of SACS. Both, cross section and PFNS uncertainties are considered using Equation (7).

Reaction	$E_{50\%}$	Experiment		Mannhart		AIACHNE		$100\left(\frac{\langle\sigma\rangle^{\mathrm{AIA}}}{\langle\sigma\rangle^{\mathrm{Man}}}-1\right)$
ID	(MeV)	$\langle\sigma\rangle$ (mb)	δ (%)	$\langle\sigma\rangle$ (mb)	δ (%)	$\langle\sigma\rangle$ (mb)	δ(%)	(%)
^{197}Au(n,γ)	0.72	75.5(1.0)	1.3	75.0(7)	0.9	74.8(7)	1.0	0.26
^{181}Ta(n,γ)	0.82	87.3(1.2)	1.4	83.5(4.5)	5.4	83.2(4.5)	5.4	–0.28
^{63}Cu(n,γ)	0.96	10.3(3)	2.9	10.41(90)	8.7	10.39(90)	8.6	–0.20
^{235}U(n,f)	1.70	1210(15)	1.2	1227(15)	1.2	1225(17)	1.4	–0.07
^{239}Pu(n,f)	1.77	1812(25)	1.4	1798(22)	1.2	1796(26)	1.5	–0.06
^{237}Np(n,f)	2.05	1361(22)	1.6	1360(23)	1.7	1359(25)	1.9	–0.02
^{103}Rh(n,n')^{103m}Rh	2.38	734(20)	2.7	725(29)	4.0	725(29)	4.0	0.10
^{115}In(n,n')^{115m}In	2.67	197.4(2.8)	1.4	190.5(3.2)	1.7	190.5(3.6)	1.9	0.02
^{93}Nb(n,n')^{93m}Nb	2.69	147.5(2.5)	1.7	146.(3.8)	2.6	146.0(4.0)	2.7	0.01
^{113}In(n,n')^{113m}In	2.73	161.2(3.2)	2.0	157.(2.)	1.2	158.0(2.4)	1.5	0.01
^{238}U(n,f)	2.77	325.7(5.2)	1.6	321.5(4.1)	1.3	322.0(5.0)	1.5	0.15
^{232}Th(n,f)	3.01	84.55(1.9)	2.3	83.3(4.8)	5.8	83.5(4.9)	5.9	0.17
^{199}Hg(n,n')^{199m}Hg	3.10	298(5)	1.8	296(11)	3.7	296(11)	3.8	0.15
^{47}Ti(n,p)	3.82	19.27(33)	1.7	19.53(55)	2.8	19.57(58)	3.0	0.22
^{32}S(n,p)	4.07	72.5(2.5)	3.5	74.0(1.9)	2.6	74.0(2.0)	2.8	0.14
^{64}Zn(n,p)	4.17	40.59(65)	1.6	42.64(39)	1.9	42.78(89)	2.1	0.33
^{58}Ni(n,p)	4.20	117.5(1.5)	1.3	117.3(2.2)	1.9	117.7(2.5)	2.1	0.33
^{54}Fe(n,p)	4.44	86.84(1.1)	1.3	86.4(2.8)	3.2	86.7(2.9)	3.3	0.28
^{204}Pb(n,n')^{204m}Pb	5.04	20.87(73)	3.5	20.37(96)	4.7	20.44(98)	4.8	0.34
^{27}Al(n,p)	5.84	4.88(10)	2.1	4.74(11)	2.4	4.74(12)	2.6	0.01
^{59}Co(n,p)	5.94	1.69(4)	2.5	1.713(65)	3.8	1.713(68)	4.0	0.03
^{46}Ti(n,p)	6.08	14.07(25)	1.8	13.81(55)	3.4	13.84(48)	3.5	0.23
^{60}Ni(n,p)	7.06	2.73(13)	4.8	2.80(7)	2.3	2.81(7)	2.5	0.36
^{28}Si(n,p)	7.23	6.9(1)	2.0	7.10(21)	2.9	7.10(22)	3.1	–0.11
^{63}Cu(n,α)	7.27	0.689(14)	2.0	0.692(25)	3.6	0.692(26)	3.7	–0.09
^{56}Fe(n,p)	7.58	1.465(26)	1.8	1.462(45)	3.1	1.465(48)	3.3	0.16
^{238}U(n,2n)	8.21	19.2(1.9)	10	21.1(1.1)	5.4	21.1(1.2)	5.6	0.19
^{24}Mg(n,p)	8.26	1.996(48)	2.4	2.101(37)	1.8	2.099(22)	2.1	–0.10
^{48}Ti(n,p)	8.35	0.425(8)	1.9	0.426(28)	6.5	0.427(28)	6.6	0.26
^{59}Co(n,α)	8.37	0.222(4)	1.9	0.221(22)	10	0.221(22)	10	0.18
^{27}Al(n,α)	8.67	1.016(15)	1.5	1.016(19)	1.8	1.015(22)	2.1	–0.09
^{51}V(n,α)	9.98	0.039(1)	2.2	0.039(3)	8.2	0.039(3)	8.3	0.78
^{169}Tm(n,2n)	10.4	6.69(42)	6.3	6.25(24)	3.8	6.24(25)	4.0	–0.16
^{93}Nb(n,2n)^{93m}Nb	11.3	0.791(40)	5.1	0.790(19)	2.4	0.787(20)	2.6	–0.28
^{127}I(n,2n)	11.6	2.069(56)	2.7	2.102(81)	3.9	2.101(92)	4.0	–0.03
^{65}Cu(n,2n)	12.7	0.658(14)	2.2	0.653(23)	3.5	0.655(23)	3.4	0.30
^{55}Mn(n,2n)	12.9	0.482(19)	3.9	0.473(19)	4.0	0.473(18)	3.8	0
^{59}Co(n,2n)	13.1	0.405(10)	2.5	0.408(16)	3.7	0.408(14)	3.5	0.05
^{63}Cu(n,2n)	13.8	0.184(7)	4.0	0.199(9)	4.5	0.199(8)	3.9	0.30
^{89}Y(n,2n)	13.9	0.341(12)	3.5	0.346(16)	4.5	0.348(14)	3.9	0.69
^{89}Y(n,2n)	13.9	0.351(13)	3.7	0.346(16)	4.5	0.348(14)	3.9	0.69
^{19}F(n,2n)	14.1	0.0161(5)	3.4	0.0163(9)	5.6	0.0165(8)	4.8	1.23
^{90}Zr(n,2n)	14.4	0.221(6)	2.9	0.218(12)	5.4	0.220(9)	4.3	0.83
^{58}Ni(n,2n)	15.0	0.0086(3)	3.6	0.0086(6)	6.8	0.0088(4)	4.8	1.16
^{23}Na(n,2n)	15.6	0.0087(3)	3.5	0.0086(7)	8.5	0.0087(5)	5.2	0.87
^{23}Na(n,2n)	15.6	0.0090(3)	3.6	0.0086(7)	8.5	0.0087(5)	5.2	0.87
^{169}Tm(n,3n)	18.5	0.0145(9)	6.2	0.0147(45)	30	0.0150(12)	7.9	2.04

^{6}Li and Dyachenko et al. PFNS, and adopt instead Blinov et al., 1980, Boytsov et al. anthracene and thin-wall ionization chamber, and final Lajtai et al. data. Boldeman, ^{6}Li and Dyachenko et al. PFNS data suffered from not fully resolving the ^{6}Li peak in the detector response, while final Lajtai et al. data resolved those issues for the latter

measurement. The Boytsov measurements, on the other hand, did not employ ^{6}Li nuclear data for their analysis. While Blinov, 1980 et al. PFNS analysis relied on ^{6}Li nuclear data and show a distinct decrease in the PFNS around the ^{6}Li peak (Fig. 2), we rejected all data around the ^{6}Li peak for the evaluation.

The evaluated mean energy from this pointwise evaluation is 2.13 MeV, while it is 2.11 MeV for Mannhart's (pointwise). Smoothing this evaluation changes the mean energy by only 0.002%. On the contrary, the mean energy calculated from the IRDFF smoothed Mannhart evaluation is 0.6% higher (2.12 MeV). The smoothing algorithm used for IRDFF data removed more aggressively structures in Mannhart's pointwise evaluation below 1 MeV leading to the larger discrepancies in mean energies. The evaluated mean energy uncertainties are 9.36 keV versus 7.95 keV for this versus Mannhart's evaluation after enforcing the normalization constraint on the PFNS and the covariances following equations (3)–(6) of Ref. [42]. The normalization constraint requires that the integral over the PFNS for energies where it is non-negligible be unity and the rows and columns of covariances sum to zero.

The normalized new evaluated uncertainties in the right-hand side of Figure 14 are smaller than those of Mannhart (also satisfying the normalization constraint) below 3 MeV as we include Blinov et al. and Boytsov et al. PFNS that were not included in the latter evaluation. On the contrary, they are larger from 3–9 MeV, where our estimated uncertainties for Blinov, 1973 et al., Böttger et al., and Poenitz et al. are larger. Enforcing the normalization constraint on the covariances leads to reduced evaluated uncertainties and areas of negative and positive correlations in the evaluated covariances (Fig. 15) as is expected and was illustrated, for instance, in Ref. [42].

4.3 Validation with spectrum averaged cross sections

SACS in the ^{252}Cf(sf) neutron spectrum were calculated from Mannhart's PFNS and the new smoothed evaluation using a log-log interpolation[6] of the spectrum for the reactions listed in Table 4. These calculated values are compared to compiled SACS experimental data as shown in Tables 18 and 19 of Ref. [48]. The differences in calculated SACS, $\langle\sigma\rangle$, between using Mannhart's and this new evaluation are very small below $E_{50\%}$ of 14 MeV (see Fig. 16). For the highest energies, the mean values calculated with the new evaluation trends slightly higher than using Mannhart's evaluation. However, SACS with the new versus Mannhart's evaluation still agree well within evaluated uncertainties. The observed deviation seems to be related to the newly added data at high energies, specifically, due to Chalupka et al. data. The observed close agreement reflects the fact that the newly evaluated PFNS is close to Mannhart's from 300 keV to 12.8 MeV and then deviates at higher energies. The average C/E (i.e., the sum over C/E divided by the number of experimental data points) deviates 0.08% and 0.34% from unity for Mannhart's evaluation, and the new evaluation, respectively.

[6] Linear interpolation of the evaluated PFNS is not appropriate due to the sparse energy grid.

5 Summary, conclusions, and outlook

Here, we re-evaluated the prompt fission neutron spectrum (PFNS) of spontaneously fissioning ^{252}Cf(sf) – a Neutron Data Standards observable. The current Standard was published by W. Mannhart in 1987, but cannot be updated as the input for this evaluation, experimental mean values and covariances, were lost. While we were able to reproduce the evaluated data of Mannhart within the experimental uncertainties of the evaluation, some open questions (most importantly regarding the correlations of input experimental covariances and the exact rejected experimental data) made it impossible to exactly reproduce Mannhart's evaluation.

The second step of this work was to provide a new ^{252}Cf(sf) PFNS evaluation. This new evaluation factors in experimental data published after Mannhart's evaluation and new knowledge on previous experiments uncovered by careful review of all experimental data entering the evaluation. The new evaluated ^{252}Cf(sf) PFNS shows fewer erratic structures than the current Standards one below 300 keV. Mannhart's evaluation below 300 keV was affected by data from Dyachenko et al. and Boldeman, ^{6}Li et al. that showed biases from incorrectly resolving the ^{6}Li peak for the detector response. We rejected both data sets and instead included data measured without ^{6}Li detectors (Boytsov et al.) or where these data were better resolved for the detector response analysis (Lajtai et al. and Blinov, 1980 et al.). The new evaluation also features an extended energy range to lower and higher outgoing neutron energies (down to 500 eV and up to 25 MeV) as Blinov, 1980 et al., Chalupka et al. and Märten, 1990 (60°) et al. data, that provide data at these energies, were included. The newly evaluated uncertainties are larger from 3–9 MeV and smaller otherwise.

Despite these changes in the ^{252}Cf(sf) PFNS, the spectrum averaged cross sections (SACS) of importance to the IRDFF community calculated with the new spectrum are very close to those calculated with Mannhart's evaluation except for those reactions with the highest threshold. Even for those, the calculated SACS agree with experimental values and calculated values using Mannhart's evaluation well within their uncertainties. Given that, this new evaluation is now a candidate for inclusion in the next release of the Neutron Data Standards.

New experimental ^{252}Cf(sf) PFNS would be especially helpful above 10 MeV, where the trend is defined by few scattered data sets. Also, measurements with other detectors than those relying on ^{6}Li would be helpful below 800 keV to counter-check the spectrum there. Both of these proposed measurement types would be challenging as the PFNS are low in the wings, affected by backgrounds and neutron detectors are often not well-characterized.

Acknowledgments

The AIACHNE team would like to thank J.W. Boldeman, A. Chalupka, H. Märten, B. Strohmaier and S. Tagesen for answering questions on their experiments. A.D. Carlson would like to thank N.V. Kornilov for answering questions on his experiments before his death.

Funding

This work was supported by the U.S. Department of Energy, Office of Science, Office of Nuclear Physics, under the Nuclear Data InterAgency Working Group Research Program. Work at LANL was carried out under the auspices of the National Nuclear Security Administration (NNSA) of the U.S. Department of Energy (DOE) under contract 89233218CNA000001. This material is partially based upon work supported by the Department of Energy National Nuclear Security Administration through the Nuclear Science and Security Consortium under Award Number DE-NA0003996. Work at Brookhaven National Laboratory was sponsored by the Office of Nuclear Physics, Office of Science of the U.S. Department of Energy under Contract No. DE-AC02- 98CH10886 with Brookhaven Science Associates, LLC.

Conflicts of interest

The authors declare that they have no competing interests to report.

Data availability statement

Data are provided as Supplementary Material. They will be also made available to the Neutron Data Standards committee for publication on the IAEA homepage and to the Nuclear Energy Agency Working Party on International Nuclear Data Evaluation Cooperation Subgroups 50 and 54 [73].

Supplementary material

The supplemental material contain seven files:

- Two files for the new pointwise evaluation (mean values and correlations) shown in Figures 14 and 15,
- Two files (mean values and correlations) for the pointwise evaluation matching Mannhart's evaluation the closest shown in Figure 13,
- Two json databases representing the input data to the before-mentioned evaluations,
- The smoothed version of the new pointwise evaluation is given in Figure 14.

The evaluated files are simple text files with the first column containing outgoing energy (MeV), the second column the PFNS, and the third column relative uncertainties in %. The spectra are not normalized, and thus the PFNS has arbitrary units. The correlation files contain for each row, a row of the covariance. The smoothed evaluation contains only a column with outgoing energy and PFNS that is now given in 1/MeV as it is normalized.

The json experimental database contains the input data as used for the evaluations. Each dataset is contained in one dictionary that contains outgoing energy, mean values, covariances along with metadata key words extracted from the literature, EXFOR and documentation of thoughts of the authors.

These files should help guarantee reproducibility of the evaluation.

The Supplementary material is available at https://www.epj-n.org/10.1051/epjn/2025061/olm.

Author contribution statement

D. Neudecker: Conceptualization, Data curation, Formal analysis, Funding acquisition, Investigation, Methodology, Project administration, Software, Supervision, Visualization, Writing – original draft, Writing – review and editing. **K.J. Kelly:** Conceptualization, Data curation, Formal analysis, Funding acquisition, Investigation, Writing – original draft, Writing – review and editing. **A.D. Carlson:** Data curation, Formal analysis, Writing – review and editing. **B. Pritychenko:** Data curation, Investigation, Validation, Writing – review and editing. **D. Brown:** Formal analysis, Funding acquisition, Investigation, Methodology, Project administration, Software, Validation, Writing – original draft, Writing – review and editing. **M.J. Grosskopf:** Data curation, Methodology, Supervision, Validation, Writing – review and editing. **S.A. Vander Wiel:** Conceptualization, Data curation, Funding acquisition, Methodology, Writing – review and editing. **R.C. Haight:** Data curation, Writing – review and editing. **R. Capote:** Data curation, Validation, Writing – original draft, Writing – review and editing. **T.N. Massey:** Formal analysis, Investigation, Writing – review and editing. **A. Trkov:** Formal analysis, Validation. **N. Walton:** Data curation, Formal analysis, Investigation, Writing – review and editing.

References

1. D.G. Madland, J.R. Nix, New calculation of prompt fission neutron spectra and average prompt neutron multiplicities, Nucl. Sci. Eng. **81**, 213 (1982)
2. G. Vladuca, A. Tudora, Improved Los Alamos model applied to the neutron induced fission of ^{239}Pu and ^{240}Pu and to the spontaneous fission of Pu isotopes, Ann. Nucl. Energy, **28**, 689 (2001)
3. R. Capote, Y.-J. Chen, F.-J. Hambsch, N.V. Kornilov, J.P. Lestone, O. Litaize, B. Morillon, D. Neudecker, S. Oberstedt, T. Ohsawa, N. Otuka, V.G. Pronyaev, A. Saxena, O. Serot, O.A. Shcherbakov, N.-C. Shu, D.L. Smith, P. Talou, A. Trkov, A.C. Tudora, R. Vogt, A.S. Vorobyev, Prompt fission neutron spectra of actinides, Nucl. Data Sheets **131**, 1 (2016)
4. D. Neudecker, P. Talou, T. Kawano, A.C. Kahler, M.C. White, T.N. Taddeucci, R.C. Haight, B. Kiedrowski, J.M. O'Donnell, J.A. Gomez, K.J. Kelly, M. Devlin, M.E. Rising, Evaluations of energy spectra of neutrons emitted promptly in neutron-induced fission of ^{235}U and ^{239}Pu, Nucl. Data Sheets **148**, 293 (2018)
5. D. Neudecker, P. Talou, T. Kawano, D.L. Smith, R. Capote, M.E. Rising, A.C. Kahler, Evaluation of the ^{239}Pu prompt fission neutron spectrum induced by neutrons of 500 keV and associated covariances, Nucl. Instrum. Methods Phys. Res. A: Accel. Spectrom. Detect. Assoc. Equip. **791**, 80 (2015)
6. N. Otuka, E. Dupont, V. Semkova, B. Pritychenko, A.I. Blokhin, M. Aikawa, S. Babykina, M. Bossant, G. Chen, S. Dunaeva, R.A. Forrest, T. Fukahori, N. Furutachi, S. Ganesan, Z. Ge, O.O. Gritzay, M. Herman, S. Hlavač, K. Katō, B. Lalremruata, Y.O. Lee, A. Makinaga,

K. Matsumoto, M. Mikhaylyukova, G. Pikulina, V.G. Pronyaev, A. Saxena, O. Schwerer, S.P. Simakov, N. Soppera, R. Suzuki, S. Takács, X. Tao, S. Taova, F. Tárkányi, V.V. Varlamov, J. Wang, S.C. Yang, V. Zerkin, Y. Zhuang, Towards a more complete and accurate experimental nuclear reaction data library (EXFOR): International collaboration between Nuclear Reaction Data Centres (NRDC), Nucl. Data Sheets **120**, 272 (2014)
7. A.D. Carlson, V.G. Pronyaev, R. Capote, G.M. Hale, Z.-P. Chen, I. Duran, F.-J. Hambsch, S. Kunieda, W. Mannhart, B. Marcinkevicius, R.O. Nelson, D. Neudecker, G. Noguere, M. Paris, S.P. Simakov, P. Schillebeeckx, D.L. Smith, X. Tao, A. Trkov, A. Wallner, W. Wang, Evaluation of the neutron data standards, Nucl. Data Sheets **148**, 143 (2018)
8. P. Talou, I. Stetcu, P. Jaffke, M.E. Rising, A.E. Lovell, T. Kawano, Fission fragment decay simulations with the CGMF code, Comput. Phys. Commun. **269**, 108087 (2021)
9. O. Litaize, O. Serot, L. Berge, Fission modelling with FIFRELIN, Eur. Phys. J. A **51**, 177 (2015)
10. J.M. Verbeke, J. Randrup, R. Vogt, Fission reaction event yield algorithm FREYA 2.0.2, Comp. Phys. Commun. **222**, 263 (2018)
11. W.J. Mannhart, Evaluation of the Cf-252 fission neutron spectrum between 0 MeV and 20 MeV, in *Properties of Neutron Sources, Proceedings of an Advisory Group Meeting on Properties of Neutron Sources Organized by the International Atomic Energy Agency and held in Leningrad, USSR, 9–13 June 1986*, number IAEA-TECDOC-410 (International Atomic Energy Agency, 1987), pp. 158–171
12. N.V. Kornilov, Verification of the ^{252}Cf standard in the energy range 2–20 MeV, Technical Report INDC(USA)-108, U.S.A. Report to the I.N.D.C., 2015
13. H. Märten, D. Richter, D. Seeliger, W.D. Fromm, R. Böttger, H. Klein, The ^{252}Cf(sf) neutron spectrum in the 5- to 20-MeV energy range, Nucl. Sci. Eng. **106**, 353 (1990)
14. A. Lajtai, P.P. Dyachenko, V.N. Kononov, E.A. Seregina, Low-energy neutron spectrometer and its application for ^{252}Cf neutron spectrum measurements, Nucl. Instrum. Methods Phys. Res. A: Accel. Spectrom. Detect. Assoc. Equip. **293**, 555 (1990)
15. S. Tagesen, A. Chalupka, L. Malek, R. Böttger, Results of a low-background measurement of the fission neutron spectrum from ^{252}Cf in the 9- to 29-MeV energy range, Nucl. Sci. Eng. **106**, 367 (1990)
16. A. Göök, F.-J. Hambsch, M. Vidali, Prompt neutron multiplicity in correlation with fragments from spontaneous fission of ^{252}Cf, Phys. Rev. C **90**, 064611 (2014)
17. E. Blain, A. Daskalakis, R.C. Block, Y. Danon, Measurement of prompt fission neutron spectrum for spontaneous fission of ^{252}Cf using γ multiplicity tagging, Phys. Rev. C **95**, 064615 (2017)
18. S.L. Bao, G.Y. Tang, J.H. Fan, W.T. Cao, Test for the corrections in the measurement of ^{252}Cf spontaneous fission prompt neutron spectrum in low energy portion, in *50 Years of Nuclear Fission Conference* (Washington D.C., 1989), Vol. 2, p. 951
19. A.D. Carlson, V.G. Pronyaev, D.L. Smith, N.M. Larson, Z. Chen, G.M. Hale, F.-J. Hambsch, E.V. Gai, S.Y. Oh, S.A. Badikov, T. Kawano, H.M. Hofmann, H. Vonach, S. Tagesen, International evaluation of neutron cross section standards, Nucl. Data Sheets **110**, 3215 (2009)
20. M.W. Herman, Covariance data in the fast neutron region, Technical Report NEA/NSC/WPEC/DOC(2010)427, Organization for Economic Co-operation and Development-Nuclear Energy Agency, 2011
21. W. Mannhart, Data fitting and evaluation techniques for neutron spectra, in *International Symposium on Nuclear Data Evaluation Methodology: Brookhaven National Laboratory, Upton, NY, USA 12–16 October 1992*, edited by Charles L. Dunford (Brookhaven National Laboratory, World Scientific Pub Co Inc, 1993), pp. 247–256
22. W.J. Mannhart, Status of the Cf-252 fission neutron spectrum evaluation with regard to recent experiments, in *Physics of Neutron Emission in Fission, Proceedings of an IAEA Consultants Meeting, Mito City, Japan, 24–227 May 1988*, number INDC(NDS)-220, Distr.: L (International Atomic Energy Agency, 1989), pp. 305–335
23. D.L. Smith, D. Neudecker, R. Capote Noy, Prompt fission neutron spectrum evaluation techniques, Technical Report INDC(NDS)-0678, International Atomic Energy Agency, 2015
24. P.P. Dyachenko, E.A. Seregina, L.S. Kutsaeva, A. Lajtai, V.N. Kononov, P.A. Androsenko, A.A. Androsenko, Absolute measurements of the prompt neutron spectrum produced by spontaneous fission of Cf-252 in the low-energy region, Vopr. At. Nauki Tekhn., Ser. Yadernye Konstanty **3**, 3 (1985)
25. P.P. Dyachenko, E.A. Seregina, L.S. Kutsaeva, A. Lajtai, V.N. Kononov, P.A. Androsenko, A.A. Androsenko, Absolute measurements of the prompt neutron spectrum produced by spontaneous fission of Cf-252 in the low-energy region, Technical report, USSR report to the I.N.D.C., translation of Vopr. At. Nauki Tekhn., Ser. Yadernye Konst., 1989, p. 3
26. R. Böttger, H. Klein, A. Chalupka, B. Strohmaier, Investigation of the spectral fluence of neutrons from spontaneous fission of ^{252}Cf by means of time-of-flight spectrometry, Nucl. Sci. Eng. **106**, 377 (1990)
27. R. Böttger, H. Klein, A. Chalupka, B. Strohmaier, The neutron energy spectrum from the spontaneous fission of Cf-252 in the energy range $2\,\mathrm{MeV} \leq \mathrm{E} \leq 14\,\mathrm{MeV}$, in *Nuclear Data for Science and Technology*, edited by K.H. Böckhoff (1983), pp. 484–487
28. R. Böttger, H.J. Brede, M. Cosack, G. Dietze, R. Jahr, H. Klein, H. Scholermann, B.R.L. Siebert, A multi-angle time-of-flight spectrometer for fast neutron scattering experiments, in *Nuclear Data for Science and Technology*, edited by K.H. Böckhoff (1983), pp. 836–839
29. R. Böttger, H. Klein, A. Chalupka, B. Strohmaier, The neutron spectrum of the spontaneous fission of Cf-252 (3–12 MeV) neutron energy, in *Properties of Neutron Sources, Proceedings of an advisory group meeting on Properties of Neutron Sources organized by the International Atomic Energy Agency and held in Leningrad, USSR, 9–13 June 1986*, number IAEA-TECDOC-410 (International Atomic Energy Agency, 1987), pp. 186–189
30. H. Märten, D. Richter, D. Seeliger, Analysis of Experimental Data on the High-energy End of the ^{252}Cf Spontaneous-fission Neutron Spectrum, Technical Report INDC(GDR)-28L, I.N.D.C., 1984
31. H. Märten, D. Seeliger, B. Stobinski, The high-energetic part of the neutron spectrum from spontaneous fission of

^{252}Cf, in *IAEA Consultants' Meeting on the ^{235}U Fast-neutron Fission Cross-section and the ^{252}Cf Fission Neutron Spectrum, Smolenice, Czechoslovakia, 28 March–1 April 1983*, number INDC(NDS)-146 (1983), pp. 195–198
32. H. Märten, D. Seeliger, B. Stobinski, The high-energetic end of the neutron spectrum from spontaneous fission of ^{252}Cf, in *Proceedings of the XIIth International Symposium on Nuclear Physics – Heavy-Ion Collisions and Nuclear Fission – November 22–26, 1982 in Gaussig (GDR), Organized by the Technical University of Dresden*, number INDC(GDR)-0026G (1982), pp. 122–124
33. H. Märten, D. Seeliger, B. Stobinski, The high-energetic Part of the Cf-252 Spontaneous-fission Neutron Spectrum, Technical Report INDC(GDR)-17, Germ. Dem. Rep. report to the I.N.D.C., 1982
34. H. Märten, D. Seeliger, B. Stobinski, The high-energetic end of the neutron spectrum from spontaneous fission of ^{252}Cf, in *Nuclear Data for Science and Technology*, edited by K.H. Böckhoff (1983), pp. 488–491
35. W.P. Poenitz, T. Tamura, Investigation of the prompt-neutron spectrum for spontaneously-fissioning ^{252}Cf, in *Nuclear Data for Science and Technology*, edited by K.H. Böckhoff (1983), pp. 465–472
36. W.P. Poenitz, The black neutron detector, Nucl. Instrum. Methods **109**, 413 (1973)
37. M.V. Blinov, G.S. Boykov, V.A. Vitenko, New experimental data on the energy spectrum of ^{252}Cf spontaneous fission prompt neutrond, in *Nuclear Data for Science and Technology*, edited by K.H. Böckhoff (1983), pp. 479–483
38. M.V. Blinov, G.S. Boykov, V.A. Vitenko, Prompt Neutron Energy Spectrum for the Spontaneous Fission of ^{252}Cf, Technical Report INDC(CCP)-238, Report to the I.N.D.C., 1984
39. O.I. Batenkov, M.V. Blinov, G.S. Boykov, V.A. Vitenko, Experimental and theoretical investigation of the energ distribution of Cf-252 spontaneous fission neutrons, in *IAEA Consultants' Meeting on the ^{235}U Fast-neutron Fission Cross-section and the ^{252}Cf Fission Neutron Spectrum, Smolenice, Czechoslovakia, 28 March–1 April 1983*, number INDC(NDS)-146 (1983), pp. 161–174
40. J. W. Boldeman, B.E. Clancy, D. Culley, Measurements of the prompt fission neutron spectrum from the spontaneous fission of ^{252}Cf, Nucl. Sci. Eng. **93**, 181 (1986)
41. M. Herman, A. Trkov, ENDF-6 Formats Manual, Technical Report BNL-90365-2009, Brookhaven National Laboratory, 2009
42. D. Neudecker, R. Capote, D.L. Smith, T. Burr, P. Talou, Impact of the normalization condition and model information on evaluated prompt fission neutron spectra and associated uncertainties, Nucl. Sci. Eng. **179**, 381 (2015)
43. M.J. Grosskopf, S. Vander Wiel, D. Neudecker, On Pathologies in Estimating the Mean with Relative Systematic Uncertainties, Technical Report LA-UR-22-32397, Los Alamos National Laboratory, 2022
44. R. Peelle, Peelle's pertinent puzzle, Informal Oak Ridge National Laboratory Memorandum, October 1987
45. S. Chiba, D.L. Smith, A suggested procedure for resolving an anomaly in least-squares data analysis known as "Peelle's Pertinent Puzzle" and the general implications for nuclear data evaluation, J. Nucl. Sci. Technol. **48**, 1 (1991)
46. D. Neudecker, ARIADNE – A program estimating covariances in detail for neutron experiments, EPJ Nuclear Sci. Technol. **4**, 34 (2018)
47. D. Neudecker, M. Devlin, R.C. Haight, K.J. Kelly, P. Marini, A.D. Carlson, J. Taieb, M.C. White, Templates of expected measurement uncertainties for prompt fission neutron spectra, EPJ Nuclear Sci. Technol. **9**, 32 (2023)
48. A. Trkov, P.J. Griffin, S.P. Simakov, L.R. Greenwood, K.I. Zolotarev, R. Capote, D.L. Aldama, V. Chechev, C. Destouches, A.C. Kahler, C. Konno, M. Koštál, M. Majerle, E. Malambu, M. Ohta, V.G. Pronyaev, V. Radulović, S. Sato, M. Schulc, E. Šimečková, I. Vavtar, J. Wagemans, M. White, H. Yashima, IRDFF-II: A new neutron metrology library, Nucl. Data Sheets **163**, 1 (2020)
49. A. Lajtai, P.P. Dyachenko, E.A. Seregina, V.N. Kononov, New evaluation of our absolute measurements of ^{252}Cf prompt fission neutron spectrum in the low energy range, in *Physics of Neutron Emission in Fission, Proceedings of an IAEA Consultants Meeting, Mito City, Japan, 24–227 May 1988*, number INDC(NDS)-220, Distr.: L (International Atomic Energy Agency, 1989), pp. 175–179
50. M.V. Blinov, V.A. Vitenko, V.I. Jurevich, The Measurement of the Spontaneous Fission Neutron Spectrum for ^{252}Cf, Technical Report INDC(CCP)-195, Report to the I.N.D.C., 1983
51. A.A. Boytsov, B.I. Starostov, High precision prompt neutron spectrum measurement from ^{252}Cf spontaneou s fission in the energy range 0.01–3 MeV, in *6. All-Union Conf. on Neutron Physics, Kiev, 2–6 Oct. 1983* (1983), pp. 298–300
52. B.I. Starostov, V.N. Nefedov, A.A. Bojtsov, Prompt Neutron Spectra from Fission of ^{233}U, ^{235}U and ^{239}Pu by Thermal Neutrons and from Spontaneous Fission of ^{252}Cf in the 0.01–12 MeV Energy Range, Technical Report INDC(CCP)-293, Report to the I.N.D.C., 1985
53. P. Talou, 2016, private communication between A.D. Carlson and P. Talou on Oct. 6, 2016 (by email)
54. R. Kinsey (compiled), ENDF-201 ENDF/B Summary Document, Technical Report BNL-NCS-17541, Brookhaven National Laboratory, 1979
55. G. Dietze, H. Klein, NRESP4 and NEFF4, Monte Carlo Codes for the Calculation of Neutron Response Functions and Detection Efficiencies for NE-213 Scintillation Detectors, Technical Report ND-22, Physikalisch-Technische Bundesanstalt, 1982
56. J.W. Boldeman, D.D. Culley, R.J. Cawley, The fission neutron spectrum from the spontaneous fission of ^{252}Cf, Trans. Am. Nucl. Soc. **32**, 733 (1979)
57. W. Mannhart, Status of the Evaluation of the Neutron Spectrum of ^{252}Cf(sf), Presentation available on https://www-nds.iaea.org/standards-cm-oct-2008/6.PDF, October 2008
58. D. Neudecker, T.N. Taddeucci, R.C. Haight, H.Y. Lee, M.C. White, M.E. Rising, The need for precise and well-documented experimental data on prompt fission neutron spectra from neutron-induced fission of ^{239}Pu, Nucl. Data Sheets **131**, 289 (2016)
59. S. Agostinelli et al., GEANT4 – A simulation toolkit, Nucl. Instrum. Methods Phys. Res. A **506**, 250 (2003)
60. H. Klein, F.D. Brooks, Scintillation detectors for fast neutrons, in *Proceedings of the Conference FNDA2006, International Workshop on Fast Neutron Detectors, University of Cape Town, South Africa* (Citeseer, 2006)

61. N.A.W. Walton, D. Neudecker, S.A. Vander Wiel, M.J. Grosskopf, K.J. Kelly, Machine learning-assisted identification of potential sources of bias in measurements of prompt-fission neutron spectra, Manuscript submitted for publication, 2025
62. N.V. Kornilov, I. Fabry, S. Oberstedt, F.-J. Hambsch, Total characterization of neutron detectors with a ^{252}Cf source and a new light output determination, Nucl. Instrum. Methods Phys. Res. A: Accel. Spectrom. Detect. Assoc. Equip. **599**, 226 (2009)
63. N.R. Stanton, A Monte Carlso Program for Calculating Neutron Detection Efficiencies in Plastic Scintillators, Technical Report COO-1545-92, Ohio State University, 1971
64. V.V. Verbinski, W.R. Burrus, T.A. Love, W. Zobel, N.W. Hill, R. Textor, Calibration of an organic scintillator for neutron spectrometry, Nucl. Instrum. Methods **65**, 8 (1968)
65. J. Grundl, C. Eisenhauer, Fission reaction rate standards and applications, in *Neutron Standards and Applications, Proceedings of a Symposium, Gaithesburg, MD, March 28–31, 1977*, number NBS-493 (1977), pp. 161–174
66. R.A. Cecil, B.D. Anderson, R. Madey, Improved predections of neutron detection efficiency for hydrocarbon scintillators from 1 MeV to about 300 MeV, Nucl. Instrum. Methods **161**, 439 (1979)
67. H. Märten (private communication, March 2023)
68. A. Chalupka, B. Strohmaier, H. Klein, R. Boettger, Properties of fission fragment detectors for tof measurements, in *IAEA Consultants' Meeting on the Cf-252 Fission Neutron Spectrum, Smolenice, Czechoslovakia, 28 March–1April 1983*, number INDC(NDS)-146 (1983), pp. 187–189
69. K.J. Kelly, M. Devlin, J.M. O'Donnell, J.A. Gomez, D. Neudecker, R.C. Haight, T.N. Taddeucci, S.M. Mosby, H.Y. Lee, C.Y. Wu, R. Henderson, P. Talou, T. Kawano, A.E. Lovell, M.C. White, J.L. Ullmann, N. Fotiades, J. Henderson, M.Q. Buckner, Measurement of the ^{239}Pu(n, f) prompt fission neutron spectrum from 10 keV to 10 MeV induced by neutrons of energy 1–20 MeV, Phys. Rev. C **102**, 034615 (2020)
70. K.J. Kelly, J.A. Gomez, M. Devlin, J.M. O'Donnell, D. Neudecker et al., Measurement of the ^{235}U(n,f) prompt fission neutron spectrum from 10 keV to 10 MeV induced by neutrons of energy 1–20 MeV, Phys. Rev. C **105**, 044615 (2022)
71. A. Savitzky, M.J.E. Golay, Smoothing and differentiation of data by simplified least squares procedures, Anal. Chem. **36**, 1627 (1964)
72. P. Virtanen, R. Gommers, T.E. Oliphant, M. Haberland, T. Reddy, D. Cournapeau, E. Burovski, P. Peterson, W. Weckesser, J. Bright, S.J. van der Walt, M. Brett, J. Wilson, K.J. Millman, N. Mayorov, A.R.J. Nelson, E. Jones, R. Kern, E. Larson, C.J. Carey, İ. Polat, Y. Feng, E.W. Moore, J. VanderPlas, D. Laxalde, J. Perktold, R. Cimrman, I. Henriksen, E.A. Quintero, C.R. Harris, A.M. Archibald, A.H. Ribeiro, F. Pedregosa, P. van Mulbregt, SciPy 1.0 Contributors, SciPy 1.0: Fundamental algorithms for scientific computing in python, Nat. Methods **17**, 261 (2020)
73. A. Lewis, D. Neudecker, A. Koning, D. Barry, J. Brown, G. Schnabel, WPEC SG50: Developing an automatically readable, comprehensive and curated experimental nuclear reaction database, EPJ Web Conf. **284**, 18003 (2023)

Cite this article as: D. Neudecker, K.J. Kelly, A.D. Carlson, B. Pritychenko, D. Brown, M.J. Grosskopf, S.A. Van der Wiel, R.C. Haight, R. Capote, T.N. Massey, A. Trkov, and N.A.W. Walton. Re-evaluating the prompt fission neutron spectrum of spontaneously fissioning ^{252}Cf, EPJ Nuclear Sci. Technol. **11**, 70 (2025). https://doi.org/10.1051/epjn/2025061